

University of Windsor

Scholarship at UWindor

Electronic Theses and Dissertations

Theses, Dissertations, and Major Papers

1-1-2007

Investigating positional changes of the Guyana Coast using Thematic Mapper (TM) and Enhanced Thematic Mapper (ETM+) imagery.

Daniel T.A. Fister
University of Windsor

Follow this and additional works at: <https://scholar.uwindsor.ca/etd>

Recommended Citation

Fister, Daniel T.A., "Investigating positional changes of the Guyana Coast using Thematic Mapper (TM) and Enhanced Thematic Mapper (ETM+) imagery." (2007). *Electronic Theses and Dissertations*. 7140. <https://scholar.uwindsor.ca/etd/7140>

This online database contains the full-text of PhD dissertations and Masters' theses of University of Windsor students from 1954 forward. These documents are made available for personal study and research purposes only, in accordance with the Canadian Copyright Act and the Creative Commons license—CC BY-NC-ND (Attribution, Non-Commercial, No Derivative Works). Under this license, works must always be attributed to the copyright holder (original author), cannot be used for any commercial purposes, and may not be altered. Any other use would require the permission of the copyright holder. Students may inquire about withdrawing their dissertation and/or thesis from this database. For additional inquiries, please contact the repository administrator via email (scholarship@uwindsor.ca) or by telephone at 519-253-3000ext. 3208.

**Investigating Positional Changes of the Guyana Coast Using Thematic Mapper (TM) and
Enhanced Thematic Mapper (ETM+) Imagery**

by

Daniel T.A. Fister

**A Thesis
Submitted to the Faculty of Graduate Studies and Research
through the Department of Geography
in Partial Fulfilment of the Requirements for
the Degree of Master of Arts at the
University of Windsor
Windsor, Ontario, Canada**

© 2007 Daniel Fister



Library and
Archives Canada

Bibliothèque et
Archives Canada

Published Heritage
Branch

Direction du
Patrimoine de l'édition

395 Wellington Street
Ottawa ON K1A 0N4
Canada

395, rue Wellington
Ottawa ON K1A 0N4
Canada

Your file *Votre référence*
ISBN: 978-0-494-42331-8
Our file *Notre référence*
ISBN: 978-0-494-42331-8

NOTICE:

The author has granted a non-exclusive license allowing Library and Archives Canada to reproduce, publish, archive, preserve, conserve, communicate to the public by telecommunication or on the Internet, loan, distribute and sell theses worldwide, for commercial or non-commercial purposes, in microform, paper, electronic and/or any other formats.

The author retains copyright ownership and moral rights in this thesis. Neither the thesis nor substantial extracts from it may be printed or otherwise reproduced without the author's permission.

AVIS:

L'auteur a accordé une licence non exclusive permettant à la Bibliothèque et Archives Canada de reproduire, publier, archiver, sauvegarder, conserver, transmettre au public par télécommunication ou par l'Internet, prêter, distribuer et vendre des thèses partout dans le monde, à des fins commerciales ou autres, sur support microforme, papier, électronique et/ou autres formats.

L'auteur conserve la propriété du droit d'auteur et des droits moraux qui protègent cette thèse. Ni la thèse ni des extraits substantiels de celle-ci ne doivent être imprimés ou autrement reproduits sans son autorisation.

In compliance with the Canadian Privacy Act some supporting forms may have been removed from this thesis.

Conformément à la loi canadienne sur la protection de la vie privée, quelques formulaires secondaires ont été enlevés de cette thèse.

While these forms may be included in the document page count, their removal does not represent any loss of content from the thesis.

Bien que ces formulaires aient inclus dans la pagination, il n'y aura aucun contenu manquant.


Canada

ABSTRACT

In an attempt to provide a timely and efficient method of coastline extraction the use of Thematic Mapper (TM) and Enhanced Thematic Mapper Plus (ETM+) data were used to delineate a 170 km stretch of the coast for 1992 and 2002 respectively. A series of preprocessing techniques, geometric correction and radiometric correction were applied to the images using the Idrisi Kilimanjaro (14.002 version) remote sensing software package. The acquisition of 25 control points along the coast ensured the geometric integrity of the 1992 and 2002 images by registering a RMS of 6.75 metres. Shorelines for both years under study were successfully exported into the ARCVIEW 9.0 GIS (ESRI, 2001) after subjecting the images to: band ratioing (band 2/band 4 and band 2/band 5), histogram thresholding (band 5), image multiplication, and raster to vector conversions.

Through overlay analysis a tabulation of the polygons which have been identified as either accretional or erosional demonstrated that the entire coastal area is one where either erosion or accretion is occurring. When the ArcGIS-generated polygons were tabulated in an Excel spreadsheet it was found that there were 2 098 accretional polygons and 2 109 erosional polygons. Only 14 polygons indicated areas of no change. These results indicate that coast displays distinct temporal phase shifts occurring at various spatial scales. Given the fact that temporal patterns of accretion and erosion have a direct influence on the morphological stability and positional shifts of the coastline it becomes vital to understand and predict these positional shifts. The results of this study provide adequate evidence that the use of TM and ETM+ imagery can make a substantial contribution to understanding, on a timely basis, the dynamic nature of the Guyana coast.

DEDICATION

I dedicate this thesis to my father the late Stanley Fister (Bachelor of Arts - Assumption University, 1960). His vision of a better life for his family was embedded in the roots of on-going education and scholarly pursuits.

ACKNOWLEDGEMENTS

I wish to thank and acknowledge the love and support of my wife, Patrizia. Without her guidance, patience and encouragement I would not have kept the passion to complete my studies. For this I will always be thankful.

I would like to extend my deepest appreciation to my advisor and mentor Dr. V. Chris Lakhan for his continual support throughout this study. His guidance, encouragement and insight has been an inspiration to me throughout my academic career. My sincere thanks to Dr. Placido LaValle for his support throughout my undergraduate and graduate studies and in particular for his advice and feedback. Also, my thanks to Dr. Rajesh Seth for his academic input and advice in the completion of the thesis. A special word of thanks to Dr. Alan Trenhaile who contributed significantly to my undergraduate studies and experience.

Lastly, I wish to thank the following officials and individuals in Guyana for their assistance in map collection and data acquisition: Mohandatt Goolsarran, Philip Kartick, Navin Chandarpal (Ministry of Science and Technology), Zakir Yamin and Mohan Mangal. Your support in the field and various research activities is most appreciated.

TABLE OF CONTENTS

ABSTRACT.....	iii
DEDICATION.....	iv
ACKNOWLEDGEMENTS.....	v
LIST OF TABLES.....	viii
LIST OF FIGURES.....	ix

CHAPTER

1.0 INTRODUCTION.....	1
1.1 Statement of the Problem.....	2
1.2 Study Area.....	4
2.0 REVIEW OF THE LITERATURE.....	7
2.1 Historical Techniques Used to Monitor Coastline Positional Change.....	7
2.2 Use of Remote Sensing Imagery to Monitor Coastline Positional Change.....	10
2.3 Investigating Coastline Positional Change with TM and ETM+ Imagery.....	14
3.0 METHODOLOGY.....	18
3.1 Objectives.....	18
3.2 Data Acquisition and Preprocessing.....	18
3.2.1 Data Acquisition.....	18
3.2.2 Data Preprocessing.....	20
3.2.3 Geometric Corrections.....	20
3.2.4 Projection of All Image Files for 1992 and 2002 to UTM.....	20
3.2.5 Mask Creation.....	21
3.3 Preprocessing with IDRISI.....	22
3.3.1 Geometric Correction.....	24
3.3.2 Projection of All Image Files for 1992 and 2002 to UTM-21N ...	31
3.3.3 Creation of Mask File for the Background.....	32
3.4 Description of General Methodology and Principles.....	36
3.4.1 Radiometric Correction - An Overview.....	38
3.4.2 Band Ratioing.....	39
3.4.3 Histogram Thresholding.....	40
3.4.4 GIS Input and Analysis.....	43

4.0	ANALYSIS	44
4.1	Radiometric Correction.....	44
4.1.1	1992 Image.....	44
4.1.2	2002 Image.....	46
4.2	Image Processing According to Methodological Principles.....	49
4.2.1	Obtaining Image 1 for 1992.....	49
4.2.2	Obtaining Image 1 for 2002.....	53
4.2.3	Obtaining Image 2 for 1992.....	55
4.2.4	Obtaining Image 2 for 2002.....	63
4.2.5	Multiplication of Image 1 and Image 2.....	70
4.2.6	Raster Clean Up Using ARCSCAN.....	74
4.2.7	Prepare New Feature Layers for Difference Imaging.....	80
5.0	RESULTS AND DISCUSSION	84
6.0	CONCLUSION	95
	REFERENCES.....	101
	VITA AUCTORIS.....	106

LIST OF TABLES

Table		Page
1	TM Bands.....	19
2	ETM+ Bands.....	19
3	ETM+ 7 Spectral Range Values in Low Gain Mode.....	47
4	ETM+ 7 Spectral Range Values in High Gain Mode	47

LIST OF FIGURES

Figure		Page
1	The Coastal Location of Guyana	4
2	Demerara East Coast - Coastlines for 1783, 1953 and 1970	6
3	Sample Landsat Image (Band 3, 1992).....	21
4	Composite Image of September 19, 1992.....	22
5	Composite Image of October 1, 2002	23
6	Collection Editor Window Showing Raster Group File Members	25
7	Composite Image for 1992.....	26
8	Composite Image for 2002.....	26
9	Reference Parameters Window Used in Resample Module	27
10	Resample Window Showing Two Composite Images for 1992 and 2002	28
11	First Ground Control Point Shown in the Input and Output Reference Images.....	29
12	Four Ground Control Points Showing the Total RMS Error	29
13	Resample Window Showing CGPs on Both Reference Images.....	31
14	Sample Landsat Image for the Study Area	33
15	Reclass Window Showing the Reclassification Values for the Mask File	34
16	Mask Image for Background (0 = Black, the background) 1 = Red.....	35
17	Flowchart for Extracting Coastlines from Images	37
18	Sample Histogram Showing Two Peaks.....	41
19	Band 2, 1992: Convert DN Values to Radiance	45
20	Band 2, 1992 After Using Radiance Module and Stretch Module	45
21	Band 2, 2002: Convert DN Values to Radiance	46
22	Band 2, 2002 After Using Radiance Module and Stretch Module	48
23	Band 5, 1992 Radiometrically Corrected and Stretched.....	49
24	Histogram for 1992_b5_rad_stre Showing Two Peaks	50
25	Reclassified Image 1992_b5_rad_stre_3classes_Image1 Showing Land/Water Boundary	52
26	Band 5, 2002	53
27	Band 5, 2002 Showing the Major Cloud Area Updated with the Values of Water Pixels.....	54
28	Histogram for 2002_b5_remove_cloud_rad_stre Showing 2 Peaks.....	54
29	Reclassified Image for Band 5, 2002 Showing the Land/Water Boundary	55
30	Band 4, 1992 (1992_b4_rad_stre).....	56
31	Overlay Window for Band 2 / Band 4 for 1992.....	57
32	1992_b2_div_b4	57
33	1992_b2_div_b5	58
34	Histogram for 1992 Band 2 / Band 4	59
35	Histogram for 1992 Band 2 / Band 5	59
36	Image Calculator Window to Evaluate the Expression: 1992_b2_div_b4>1	60
37	Band 2 / Band 4 > 1	61
38	Band 2 / Band 5 > 1	61

LIST OF FIGURES (cont'd)

Figure	Page
39	Image 2 Derived From (Band 2 / Band 4 > 1 AND Band 2 / Band 5 > 1) 61
40	Reclassified Image 2 62
41	Band 2, 2002 (2002_b2_rad_stre)..... 63
42	Band 4, 2002 (2002_b2_rad_stre)..... 64
43	Band 5, 2002 (2002_b5_remove_cloud_rad_stre)..... 64
44	Overlay Window for Band 2 / Band 4 for 2002..... 65
45	2002_b2_div_b4 65
46	2002_b2_div_b5_cldrmv 66
47	Histogram for 2002 Band 2 / Band 4 66
48	Histogram for 2002 Band 2 / Band 5 67
49	Image Calculator Window to Evaluate the Expression: 2002_b2_div_b4>1.6....68
50	Band 2 / Band 4 > 1.6 68
51	Band 2 / Band 5 > 1.25 69
52	Image 2 Derived From (Band 2 / Band 4 > 1.6 AND Band 2 / Band 5 > 1.2.) 69
53	1992 Image Derived from Multiplying Images 1 and 2 70
54	1992 Final Image File Ready for Conversion to a Vector File..... 71
55	2002 Image Derived from Multiplying Images 1 and 2 72
56	2002 Final Image File Ready for Conversion to a Vector File..... 73
57	Raster Image for 1992..... 74
58	1992 Image Showing 2 Colours..... 75
59	Raster Cleanup Menu..... 76
60	Cleaned Raster Image for 1992..... 76
61	Vector File Showing Land Polygons for 1992 77
62	Raster Image for 2002..... 78
63	2002 Image Showing 2 Colours..... 79
64	Cleaned Raster Images for 2002 79
65	Vector File Showing Land Polygons for 2002 80
66	Shoreline_1992_Union Showing Water Polygon..... 81
67	Shoreline_2002_Union Showing Water Polygon..... 81
68	Attribute Table for Difference Image 82
69	Portion of Attribute Table Showing Gridcode..... 83
70	Areas of Erosion and Accretion along the Guyana Coast..... 84
70a	Areas of Erosion and Accretion along the Guyana Coast (enlarged version) 85
71	Erosion of Papaw Beach and Ille Beach between 1992 and 2002 86
72	Accreting Band of Sediment (mouth of Pomeroon River) 87
73	Coastal Erosion Zone, Freetown to Land of Promise 88
74	Accretion Zone found along western side of mouth of the Essequibo River 89
75	Accretionary Areas, from community of Paradise to Ann's Grove..... 91
76	Accretion Areas, from Clonbrook to Concord..... 92
77	Areas of Accretion and Erosion Along the Guyana Coast 93

1.0 INTRODUCTION

The coastal zone of the world accounts for 8% of the world's surface where more than 50% of the world's population live within 60 km of this water-land boundary (Lucas, 1996). The social, economic and environmental significance of the littoral zone is of great interest to coastal planners and managers. In particular, the below sea-level coast of Guyana is home to approximately 90% of the country's population and is plagued by a series of issues including resource depletion, habitat losses, pollution, environmental degradation, flooding, erosion, salinization, and inundation (Lakhan, 2005). According to Lakhan (1994), these problems are the result of uncoordinated, individualistic and ill-conceived planning and development strategies that have negatively impacted the coastal inhabitants of Guyana.

Sixty percent of the coastal zone of Guyana is protected by some form of sea defence (earthen dams, concrete dikes, and boulder slopes). However, the coast is vulnerable to flooding due to breaches in the integrity of existing structures and a combination of factors including: mangrove forest depletion caused by the demand for wood fuel and the choking of silt mud, an increase in storms, future rise in sea level and the lack of maintenance of existing engineering structures (Singhroy, 1996). This threat to the coastal zone of Guyana would pose serious social and economic hardship as outlined by Singhroy (1996, p.1), 'It is estimated that future large-scale flooding could destroy almost \$1 billion (U.S.) of economic activity in the coastal areas.' In an effort to provide successful strategies for sound coastal management, the need for timely and

accurate coastal data is essential for an integrated management approach for the coastal resources along the Guyana coastline.

The acquisition of remotely sensed data and its subsequent integration into a Geographical Information System (GIS) has become an advantageous technique used in the detection of shoreline change. Hence, remote sensing provides an excellent aerial surveillance of a study area that when coupled with traditional modes of data acquisition assist in the process of research and analysis, as noted by Williams and Lyon (1997, p. 375), "Because GIS is a convenient tool for manipulation of mapped data, it simplified development of data sets that could be used in data analysis." Ultimately, this study will show that the use of TM and ETM+ imagery and its incorporation into a GIS is a sound and timely method in the investigation of shoreline change along the coast of Guyana.

1.1 Statement of the Problem

The social and economic importance of the coastal zone is apparent to the approximate 675 000 coastal inhabitants of Guyana. In order to provide a comprehensive strategy for the protection and development of all coastal resources, the need for timely coastal data is a requisite tool in the analysis of coastal change. The need for a comprehensive method of shoreline extraction is necessary in the investigation of coastal change for the country of Guyana. The ability to identify areas of accretion and erosion along the coast will permit investigators to assess the level of vulnerability and the corresponding management response to a specific area. Given the need to provide an

integrated approach to the successful management of the country's coastal resources, this research is of significance because it will help to establish the utility of TM and ETM+ imagery as a sound and timely approach for the detection of coastline positional changes.

In particular, the use of TM and ETM+ data will be shown to be an appropriate, efficient and cost effective means for the automatic extraction of coastlines. A synoptic view of the coastline with remote sensing will be valuable for identifying and visualizing spatial locations experiencing coastal changes. Within a GIS environment the use of multiple images derived from TM and ETM+ imagery will allow one to show areas experiencing both cumulative and isolated changes over time. Ultimately, low lying areas found along the coast need to be identified in order to provide a proactive management response for the protection of these vulnerable locations. Given this ancillary information, coastal managers can provide site-specific strategies to protect the structural integrity of existing sea defences and minimize the effects of natural and anthropogenic forces along the coast. This is especially important given the future threat of rising sea level for the coastal zone of Guyana, and all low lying countries of the world.

1.2 Study Area

The study area focuses on the Guyana coast which is a portion of the northeast coast of South America known as the Guiana Coast. The Guyana coastal plain, approximately 435 km in length, represents one of the country's major physiographic regions. The coastal plain is bordered by the Pre-Cambrian lowlands in the west and by the sandy rolling lands in the east (Figure 1). The coastal plain is generally flat and is

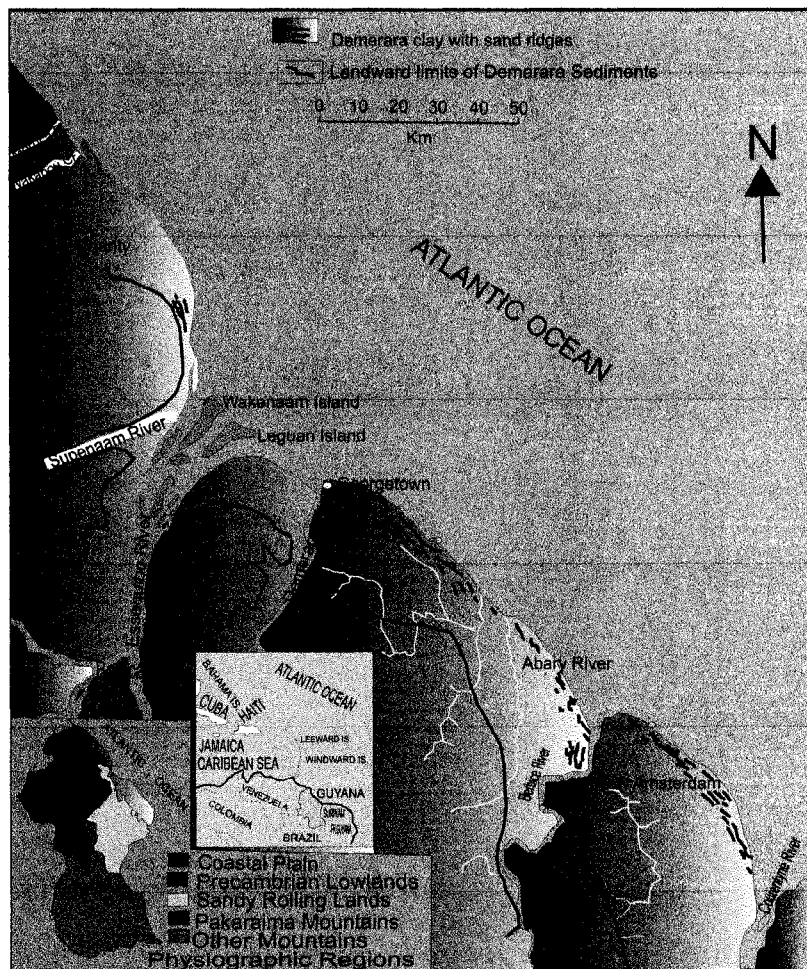


Figure 1: The Coastal Location of Guyana. Adapted from materials compiled by V.C. Lakhan.

approximately 2.5 m to 4.0 m below high tide level (Lakhan, 1991). More than 90% of the country's population live on the coastal plain which is a major source for agricultural, industrial, and recreational resources (Lakhan, 1994). Comprehensive accounts of the coast have been provided with reference to its development (Lakhan, 1994), environmental characteristics (Lakhan *et al.*, 2000, 2002) and morphology and configuration (Lakhan, 1991; Lakhan *et al.*, 2004).

The configuration and width of the coast are affected by mudbanks which migrate along the coast on a periodic basis. The movement of mudbanks is accompanied by a pattern of erosion and accretion of the adjacent coast (Allersma, 1971; Augustinus, 1987). Accretion takes place on the coast directly opposite the mudbanks, while erosion occurs along the coast opposite the troughs situated between two mudbanks. The study by Lakhan *et al.* (2004) demonstrated that the presence of mudbanks influence oscillating cyclical patterns in erosional and depositional states along the coastline. When these states occur the configuration of the coastline changes. Positional shifts in the coastline have also been documented from an analysis of the historical records and maps of the coastline. Figure 2 highlights various positional states of the coastline in the time periods 1783, 1953 and 1970. Further temporal phase shifts in sections of the Demerara coastline are also expected to occur. The study by Ahmad *et al.* (2005) found that in 2016 the coastline will exhibit positional changes in width and configuration in several locations. Understanding and predicting these changes are extremely important for planning and developmental purposes. This study will, therefore, endeavour to demonstrate that remote

sensing data could be used to identify and visualize spatial locations where changes in the position and configuration of the coastline have occurred.

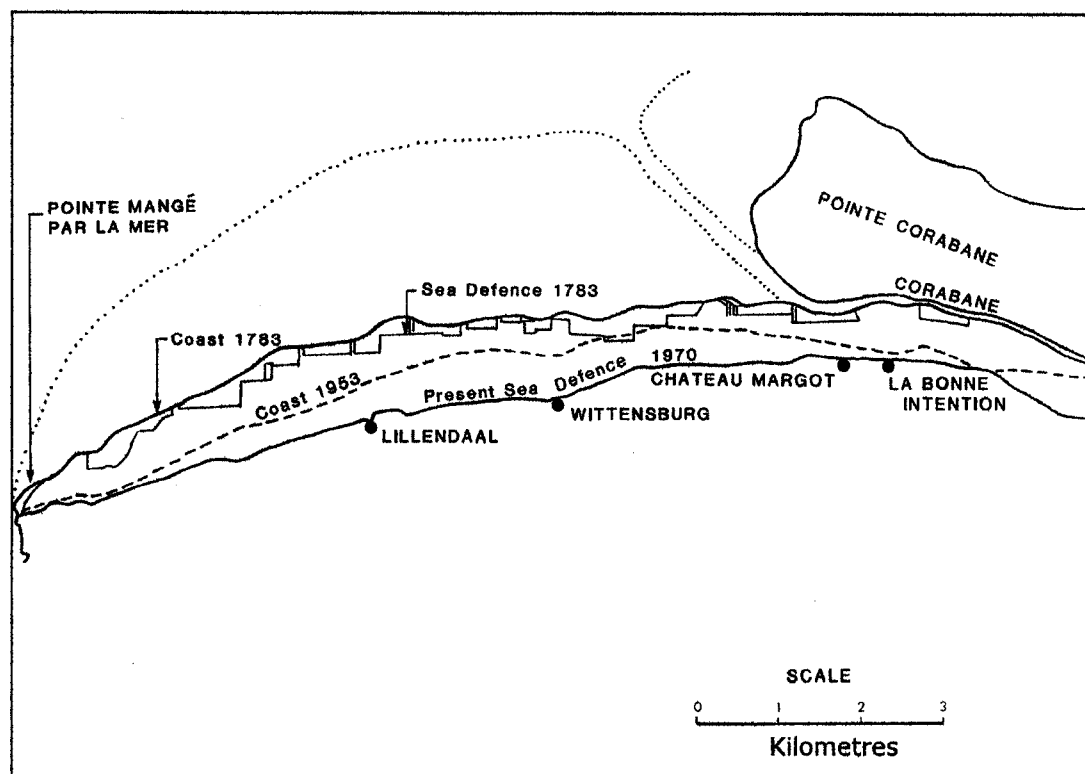


Figure 2: Demerara East Coast. Coastlines for 1783, 1953 and 1970. Redrawn from material compiled by V.C. Lakhan.

2.0 LITERATURE REVIEW

2.1 Historical Techniques Used to Monitor Coastline Positional Change

Historically, shoreline mapping has been a function of the level of sophistication of contemporary technology and methods used in determining the changing position of the coastline over time. According to Moore (2000, p. 117) technological advances have enhanced coastal research over time as,

‘Numerous shoreline mapping techniques have been developed throughout the last 27 years. The progression of techniques from manual, to partially automated, to fully automated is consistent with decreases in the cost of personal computers and workstations as well as improvements in data processing and storage capabilities.’

Prior to the 1930's, the use of planetables, alidades and rod were employed to survey the terrain and plot field measurements of the high water line (HWL) and ground control points (GCP). In an effort to standardize data collection techniques among shoreline investigators, the United States Federal Emergency Management Agency (FEMA) established draft guidelines that recommended to digitize historical and current shoreline positions from maps and aerial photographs in order to plot perpendicular transects along a shoreline for the purpose of measuring and calculating rates of shoreline change (Crowell *et al.*, 1991). Cambers (1975) employed the use of Ordnance survey maps to determine historical retreat rates of the Suffolk, England coastal cliff erosion system over a 70 to 100 year period. The subsequent use of aerial photographs provided up to date cliff top position data used in the production of paper maps which served in the calculation of annual average retreat rates (AARR).

The rate of shoreline change is one of the most common measurements used by coastal investigators to reflect the cumulative effects of morphodynamic processes that influence the coast (Dolan, *et al.*, 1991). Common sources of shoreline mapping include aerial photographs, maps (Quadrangles), nautical charts, beach profiles, topographic maps (T-sheets), and hydrographic charts (H-sheets) (Crowell, *et al.*, 1991; Dolan, *et al.*, 1991; Moore, 2000; Fletcher, *et al.*, 2003). Additionally, shoreline datums used include: high water line, approximate mean high water line, and sediment water interface (Dolan, *et al.*, 1991). Additionally, Crowell *et al.* (1991) acknowledged that the high water line (HWL) was demonstrated to be the best indicator of the land-water interface when calculating rates of shoreline change. The use of the aforementioned data sources were incorporated into paper maps and were subjected to time series analysis that measured differences in shoreline position over time.

The simplest method of rate calculation for shoreline positional change included the end point rate (EPR) which measures the distance of total shoreline movement divided by the time elapsed between measurements (Dolan, *et al.*, 1991). Variations to the EPR method include multiple shoreline position change data and their relative positions over time through the use of average of rates (AOR), linear regression (LR) and jack knifing (JK) (Dolan, *et al.*, 1991). Given the use of these spatio-temporal methods, it is believed that the prediction of future shoreline change is based upon long term shoreline behaviour in order to minimize potential random error and short term variability (Dolan, *et al.*, 1991). Fenster *et al.* (1993, p. 151) believed that linear regression models

provide, 'The most robust method for analyzing historical trends and extrapolating these trends into the future,...' through regression techniques that best fit historic data with a linear or non-linear model.

Since the 1930's the use of remotely sensed data has taken the primary form of aerial photographs (O'Regan, 1996). Modern coastal investigators continue to use aerial photographs as a data source to identify, distinguish, map and measure shoreline positional change over time using varied spatial scales. According to O'Regan (1996), the use of remotely sensed devices has successfully served to enhance coastal investigation by providing a series of benefits that include: a wide variety of spatial scales, unbiased content, repetitive coverage, and an economic and efficient method of data acquisition.

Given the utility of aerial surveillance within coastal investigation, several authors (Phillips, 1986; Foster and Savage, 1989; Smith and Zarillo, 1990; Jiménez *et al.*, 1997; Fletcher, *et al.* 2003; Al-Tahir and Ali, 2004) have incorporated aerial photographs to quantify long term and short term shoreline positional change. In particular, Jiménez *et al.* (1997, p. 1256) used aerial photography to analyse short-term shoreline changes along the Erbo Delta in Spain in order, '...to obtain a synoptic view of large coastal stretches, avoiding thus expensive and seasonal topographical beach surveys'. Subsequently, the use of aerial surveillance allowed for the formation of a base map from which future maps could be overlaid in such a fashion to allow for the detection of coastal change. The benefits provided by this method of coastal investigation include: homogeneous and

comprehensive data coverage, cost effectiveness (Gardner, 1992) and high reliability of results (Jiménez, *et al.* 1997). Jiménez, *et al.* (1997) tested the reliability of results for shoreline changes (expressed in metres per year) from both beach profile data sets and the aerial surveillance data sets, and established a linear relationship of $r = 0.98$.

The use of aerial photography and its interpretation within coastal studies has evolved in tandem with advances in imaging technology, computer hardware and software and associated peripheral devices. The level of accuracy with respect to the georeferencing of control points of a study area has progressed from projecting aerial photographs on to base topographic maps of different scales using a Zoom Transfer Scope as employed by Smith and Zarillo (1990) to digital methods. By scanning aerial photographs Al-Tahir and Ali (2004) were able to import a digital image into a Computer Aided Design (CAD) program, secure ground control points through GPS survey, georeference the images of different scales and produce images of the same reference system. Similarly, Fletcher *et al.* (2003) used vertical aerial photographs and T-sheets to determine historical shoreline positions through the digitizing of maps and aerial photographs for the sandy beaches of the Hawaiian island of Maui. During the aforementioned studies, shoreline change and its associated accretion and erosion patterns were readily identified.

2.2 Use of Remote Sensing Imagery to Monitor Coastline Positional Change

The advances made in remote sensing techniques and imaging applications have given rise to a new paradigm whereby coastal investigations are being carried out through

a variety of active and passive remote sensing methods including: light detection and ranging (LIDAR) topographic mapping, video-based coastal imaging systems and the use of satellite multi spectral sensors. By virtue of recent advances in imaging technology, LIDAR has been adopted as a joint venture by the United States Geologic Survey (USGS), National Aeronautics and Space Administration (NASA) and National Oceanic and Atmospheric Administration (NOAA) for the mapping of the United States coastline. The use of light aircraft flying at low altitudes (<1000 m) incorporates the use of differentiated GPS, internal navigation systems (INS) and inertial measuring units (IMU) with LIDAR units to scan beach widths along the coastline (Brock *et al.*, 2002). The scanning of the beaches under surveillance provides a high resolution of the terrain topography as laser light is emitted and detected by the onboard sensor given the two way travel time emitted by a laser pulse as it is reflected off a remote target (Brock *et al.*, 2002). The use of this remote sensing technique affords the coastal investigator high levels of reliability and accuracy as noted by (Brock *et al.*, 2002, p. 1),

‘Combined within contemporary airborne laser mapping systems, these newly emerged technologies now enable low cost geomorphic surveys at decimeter vertical accuracy and at spatial densities greater than 1 elevation measurement per square meter.’

Contemporary technologies provide reliable and accurate data in the production of base maps that can be fully integrated into digital form within a GIS for coastal mapping purposes and shoreline positional change analysis. The use of the video-based coastal imaging application found within the coasts of New South Wales, Australia provides a unique investigation into the diverse study of temporal scales ranging from seconds to

years, and spatial scales ranging from centimetres to kilometres (Turner *et al.*, 2006). A network of video cameras continuously monitors nearshore processes at an oblique angle as digital images are converted into three dimensional 'real world' co-ordinates from real life two dimensional video images (Turner *et al.*, 2006). The use of enhanced imaging techniques provide the framework to produce geo-referenced images that are incorporated into a coastal database for future reference and analysis (Turner *et al.*, 2006). The use of coastal imaging applications for the New South Wales coast experience has helped to shape planning and management strategies surrounding sand nourishment programs, beach protection, sand bypassing projects and coastline monitoring. This video-based coastal imaging method has proven to be a valuable asset for coastal investigators as outlined by Turner *et al.* (2006, p. 45), 'At the core of many coastal monitoring programs is the identification of the shoreline for the purposes of quantifying the available beach amenity and to assess impacts of new or existing engineering works.'

Since the launching of the Landsat 1 satellite in 1972, the use of remotely sensed images ushered in a new era of environmental monitoring as digital data began to flow from the geosynchronous orbit of space to receiving earth stations. The ensuing advantages for coastal research become apparent as outlined by O'Regan (1996, p. 193) where he states that due to the nature of the data extracted from satellite imagery, '...the data are collected in an inherently digital form, and are therefore immediately amenable to computer processing.' When the processed data are incorporated into a GIS further advantages for coastal and shoreline change detection occur, including an easy

assimilation into numerical models (O'Regan, 1996). According to Gardner (1992), the nature of data acquired from satellites allows for a continuous spatial and temporal transmission of data, as data is collected every 16 days for the study area and transmitted back as consistent digital information. This form of comprehensive coverage suggests that remotely sensed data provides a reliable and cost-effective method of spatial data acquisition for repeated observations over a broad area (Klemas, *et al*, 1993).

Furthermore, the incorporation of data into a GIS such as ARCVIEW 9.0 (ESRI, 2001) allows for future projections of shoreline change and its associated coastal management response given the utility of the overlap analysis inherent within the program. Similarly, remotely sensed data from the Landsat TM and ETM+ sensors will be incorporated into the Guyana analysis, whereby annual shoreline changes will be made from the ensuing map overlays.

The use of remotely sensed data and its incorporation into a GIS have provided an efficient and reliable data set in the detection of shoreline change. O'Regan *et al.* (1995) incorporated the use of historical shoreline data with recent data for the Te Puru coastal region of New Zealand. In the analysis, a base map from 1968 was constructed and incorporated into a GIS. Subsequently, ensuing shoreline data from 1968 was collected, digitally processed and outputted as a series of annual maps. By comparing the base map of 1968 with subsequent years, coastal researchers examined and compared shorelines between two time periods using the graphics program ARC-COAST. From the digitized data contained within the GIS, individual polygons of data from the study area were

compared and differentiated. In the analysis, positive and negative values were calculated from fixed points of the study polygons, indicating either an area of accretion or erosion respectively (O'Regan *et al.*, 1995).

More recent studies, (Grigio *et al.*, 2005; Singhroy, 2006) have employed the use of remotely sensed satellite data to map changing shoreline position and identify areas of accretion and erosion within the coastal zone. Singhroy (1996) employed the use of a combination of airborne SAR, RADARSAT and TM images for coastal mapping purposes. This method was beneficial as, 'Geomorphological mapping of Guyana's coastal plain, including detailed knowledge of erosion and depositional processes, are essential for planning sea defence strategies.' (Singhroy, 1996, p. 324). In particular, the interpretation of the remotely sensed images allowed the investigation of: sea defence priority identification in areas of severe coastal erosion; estimated coastline change; erosion, accretion and stable shorelines; land use analysis and revision among agricultural and forested lands; and risk assessment of mangrove regeneration (Singhroy, 1996). In the analysis, Singhroy demonstrated that the integration of RADARSAT and SAR images was useful in the monitoring and mapping of the coastal zone in Guyana.

2.3 Investigating Coastline Positional Change with TM and ETM+ Imagery

To ensure sustainable development within the coastal zone, the extensive survey, monitoring and database creation for all water and coastal parameters is critical. Hence, the use of satellite imagery provides data that once mapped can detect erosion and accretion processes within a coastal study area (Ahmad, 1994). Several authors (White

and El Asmar, 1999; Ryu *et al.*, 2002; Anthony *et al.*, 2002; Scott *et al.*, 2003; Alves *et al.* 2003, Noernberg and Marone, 2003; Bagli and Soille, 2004; and Grigio *et al.*, 2005) have utilized a combination of either TM and ETM+ satellite imagery in the delineation of shorelines, monitoring of coastal evolution and detection of accretion and erosion patterns. The specific benefits associated with the use of TM and ETM+ imagery for the purposes of coastline mapping include: adequate pixel resolution for medium scale mapping requirements, lower data acquisition costs (Scott *et al.*, 2003), repetitive acquisition and synoptic capabilities allowing for spatial data incorporation into a GIS, (White and El Asmar, 1999), and a more efficient method when compared to traditional geomorphological fieldwork (Noernberg and Marone, 2003). Furthermore, according to Bagli and Soille (2004), the extraction of a coastline directly from satellite images overcomes the problems associated with matching available coastal data with the image itself. This potential problem is magnified through projection system bias, mechanical error and the labourious nature of georeferencing multiple image data sets of varied scales (Bagli and Soille, 2004).

A variety of remote sensing techniques are employed by coastal investigators to delineate the boundary between open water and land to accurately determine the position of a shoreline. The proposed methodology of any coastal researcher begins with the selection of an appropriate imaging platform through which one can obtain the desired digital information as noted by Grigio *et al.* (2005, p. 412), 'The choice of the spectral bands is a very important factor in the successful interpretation of satellite images.' The

interpretation of the strip of green within the visible spectrum of TM band 2 and the near-infrared spectrum of TM band 4 has been successfully used to extract shoreline position by employing the Normalized Difference Water Index (NDWI) algorithm (McFeeters, 1996; Noernberg and Marone, 2003; Grigio et al., 2005). The NDWI, denoted by the formula - $(band\ 2 - band\ 4)/(band\ 2 + band\ 4)$, is known to enhance the differences in pixel resolution between land and sea given the fact that the typical wavelength reflectance of water is maximized at the visible end of the electromagnetic spectrum, and minimized within the near-infrared spectrum. Additionally, soil and vegetation land cover generates a maximum high reflectance of radiant energy within the near-infrared spectrum (Noernberg and Marone, 2003).

Scott *et al.* (2003) utilized Landsat 7 ETM+ imagery and the tasseled cap transformation method to extract shoreline position along the Louisiana and Delaware coastlines respectively. Based on the satellite reflectance and spectral characteristics derived from known sampling of earth terrain data, a classification system based on three components namely, brightness, greenness and wetness was developed. The transformation of this classification system was based on interpretation of the six ETM+ bands where the 'wetness' component was used to differentiate land from water (Scott *et al.*, 2003). Similarly, White and El Asmar (1999) employed the use Landsat TM data and a segmentation algorithm to delineate shoreline position along the Nile Delta, Egypt. Initially, the segmentation technique identifies known pixels of open water, referred to as 'seeds' to determine a common spectral reflectance class for water. The process merges

similar neighbouring pixels into the water classification and proceeds to grow in a homogenous grouping in all directions until dissimilar pixels are detected.

The use of Landsat TM data and its subsequent method of imaging techniques has proven to be beneficial in the investigation of coastal morphodynamics. Of particular interest is the findings by Grigio *et al.* (2005, p. 414), where the interpretation of the red, green, and blue components of the visible spectrum of TM bands 4 and 2 and its incorporation into the NDWI, ‘... provided an excellent delimitation of the coastline...’ within the study area of northeastern Brazil. After digital processing of the TM data, the coastline data was vectorized and exported into the ARCVIEW 3.0 GIS (ESRI) where polygon-based maps for three distinct time periods (1989-1998, 1998-2000, 2000-2001) were created. In the analysis, each map (polygon) was subjected to overlay analysis whereby each theme (year) was processed to ascertain areas of overlap. The union process between the themes contained within the GIS created an attribute table that presented classes for each time period and indicated the presence or absence of the shoreline position within the area of overlap along the coast. This process served to visualize and quantify areas of erosion or accretion based on the shoreline position for the period under study as sliver polygons were created through the overlay of successive shorelines.

3.0 METHODOLOGY

3.1 Objectives

With the knowledge that remotely sensed satellite data are both accurate and reliable for coastal investigation, this study will demonstrate that the use of TM and ETM+ imagery and its incorporation into a GIS are useful techniques to distinguish, differentiate, and quantify morphological change along the coast of Guyana. This thesis will, therefore, have objectives of:

- (1) utilizing remote sensing imaging techniques to delineate coastline positions from different time periods;
- (2) visualizing the spatial and temporal changes that have occurred along the coastline; and
- (3) quantifying and visualizing accretion and erosion patterns that have occurred along the coast.

3.2 Data Acquisition and Preprocessing

3.2.1 Data Acquisition

Data from two time periods was used. The data from September 19, 1992 were from the Thematic Mapper (TM) and represent seven spectral bands (see Table 1). The October 1, 2002 data were from the ETM+ sensor with seven spectral bands stretching from 0.45 micrometers to 12.5 micrometers (see Table 2).

Data for each of the time periods and for each band represented a portion of the Demerara coast and the Essequibo coast of Guyana.

Table 1: TM Bands

Bands	Wavelength (micrometers)	Wavelength (nanometers)	Resolution (meters)
1	0.45-0.52	450-520	30
2	0.52-0.60	520-600	30
3	0.63-0.69	630-690	30
4	0.75-0.90	750-900	30
5	1.55-1.75	1550-1750	30
6	10.4-12.5	10400-12500	120
7	2.08-2.35	2080-2350	30

Table 2: ETM+ Bands

Bands	Wavelength (micrometers)	Wavelength (nanometers)	Resolution (meters)
1	0.45-0.515	450-515	30
2	0.525-0.605	525-605	30
3	0.63-0.69	630-690	30
4	0.75-0.90	750-900	30
5	1.55-1.75	1550-1750	30
6	10.40-12.50	10400-12500	60
7	2.09-2.35	2090-2350	30

3.2.2 Data Preprocessing

Several image processing techniques incorporated in the Idrisi Kilimanjaro version 14.002 software (Clark Labs, 2003) were utilized to process the images. Space limitations prevent describing all the image processing techniques that were employed, but in brief those advocated by Lakhan (1993) were used to carry out the following operations.

3.2.3 Geometric Corrections

The intent of image rectification and restoration is to correct image data for distortions or degradations that stem from the image acquisition process (Lillesand and Kiefer, 1994). Geometric correction was done so that the corrected image will have the geometric integrity of a map. Distortions were corrected by analyzing well distributed ground control points (GCPs) collected along the coast of Guyana. GCPs were selected and utilized in the Resample module of Idrisi using Bilinear as the Resampling type.

3.2.4 Projection of All Image Files for 1992 and 2002 to UTM

Even though the specified coordinate system is UTM Zone 21N for both the 1992 and 2002 image files, the Project module was used on all the image bands to remove any potential anomalies or distortions that may exist in the data set. For the 1992 image bands all files were projected to the Band 2, 1992 image which was used as the reference image. For the 2002 image bands all files were projected to the Band 2, 2002 image which was used as the reference image. For both years, Bands 4 and 5 were copied and projected into the UTM Zone 21N coordinate system.

3.2.5 Mask Creation

A sample Landsat Image is shown in Figure 3. Note that the image has a black background. Normally, this background is omitted from image processing. A mask file can be used to mask out the surrounding black background box.

The Reclass module was used to create a mask image file. Using the Cursor Inquiry Mode in Idrisi, it can be verified that the entire background is black (i.e., DN = 0) whereas the other DN values range from 0-255. This can also be verified using the Histo module and examining the resulting histogram.

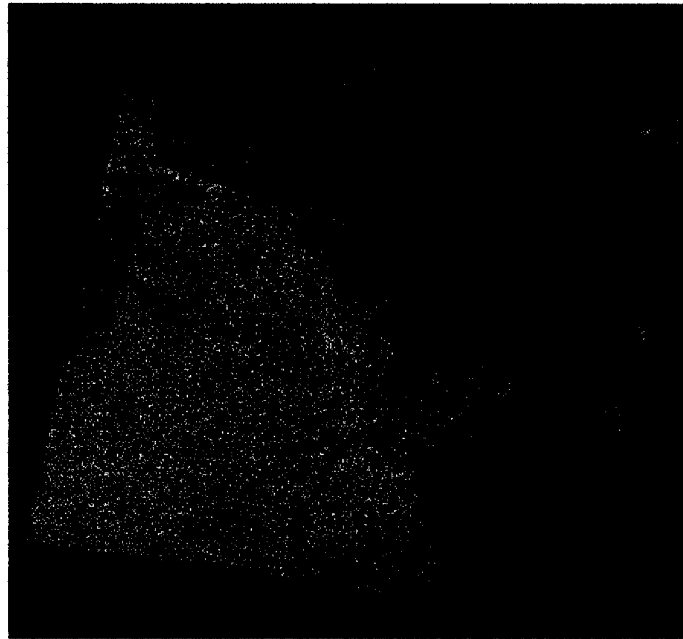


Figure 3: Sample Landsat Image (Band 3, 1992)

The Project module was used to project the Mask_for_Background file to the UTM-21N coordinate system. The Project module is available from the Reformat menu in Idrisi. The

type of file to be projected is specified as raster. The input file is specified as Mask_for_Background. The input reference system is specified as UTM-21N. The output filename is specified as Mask_for_Back_Proj.

3.3 Preprocessing of Data with IDRISI

Two Landsat images were obtained in digital format with each image stored on a separate CD. A composite image for September 19, 1992 is shown in Figure 4. A composite image for October 1, 2002 is shown in Figure 5.

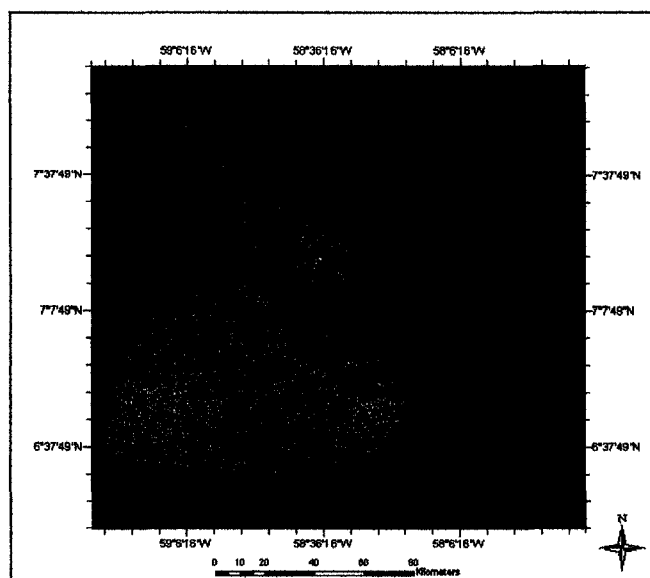


Figure 4: Composite Image of September 19, 1992

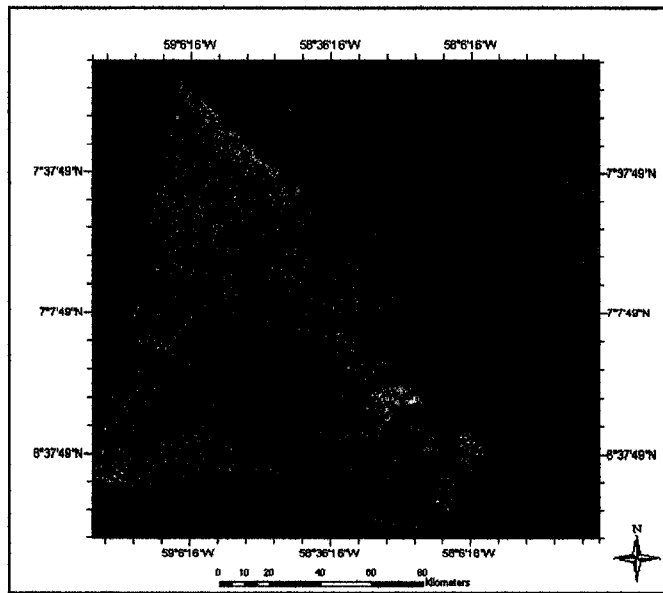


Figure 5: Composite Image of October 1, 2002

Idrisi version 14.002 was used to import the two Landsat images. A Project environment was set in Idrisi using the Project environment window available from the File menu, Data Paths. The main working folder and resource folders were designated for the software. The two images were imported into the main working folder whereas the original image files were maintained in a resource folder.

The image bands are imported into the Idrisi software and stored as Idrisi raster image files. Each Idrisi image file consists of two parts, the actual image file and a corresponding documentation file. The documentation file is used by Idrisi to display and manipulate the image. The documentation file consists of the metadata provided, resolution, and various flags which can be set for use with various Idrisi modules.

3.3.1 Geometric Correction

Idrisi's Resample module was used to perform geometric correction. In Idrisi, the Resample module can be used to register remotely sensed imagery to a grid referencing system, and make non-integer changes in the resolution of an image (Clark Labs, 2003). The Resample module is used to ensure that locations in both the 1992 and 2002 image bands correspond in the UTM coordinate reference system. The resolution of the 2002 image bands changes during the resampling process so that both images have the same resolution. The process involved in the Resampling module is one where a set of polynomial equations are developed to serve as mapping equations to transform points from the input grid to a modified output grid. The Resample module requires the selection of a mapping function, and the resampling options of either bilinear or nearest neighbor. Either of the latter two options are used to estimate, if necessary, data values in the new output grid.

To register the two images (1992 and 2002) to a common reference system, a set of well distributed ground control points were needed. Ground control points were chosen using topographic maps of the study area, and GPS data collected from field work.

In reviewing the literature it was decided that Bands 2, 4 and 5 of each image year would be used for analysis of shoreline change. Because of less cloud cover in the coastal area, the 1992 image was used as the base input reference image, and the 2002 image was chosen as the output image to be resampled. The Resample module requires the actual image bands to be resampled based on the input of ground control points. Hence, a group

file was created using Bands 2, 4 and 5 of the 2002 image using the Collection Editor in Idrisi (see Figure 6). The group file (2002grp245) allows for the resampling of all the member image bands of the group during the resample procedure. This avoids having to

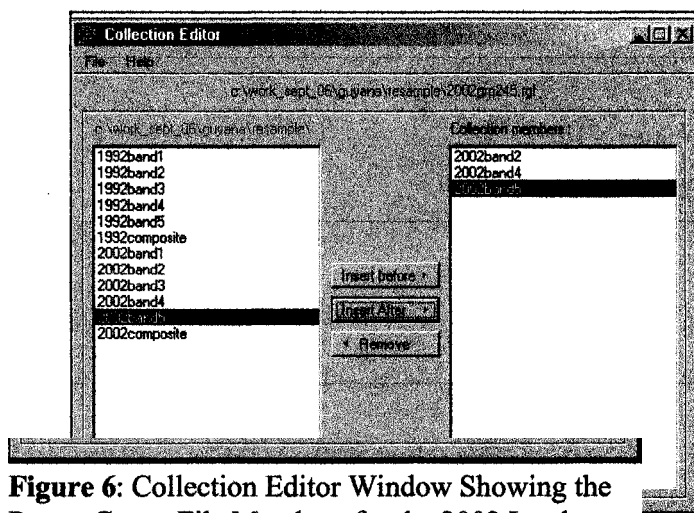


Figure 6: Collection Editor Window Showing the Raster Group File Members for the 2002 Landsat Image

run the Resample module three times, one for each image band.

In addition, the Resample module requires Input and Output reference images when placing ground control points on the images. Composite images were created for both 1992 and 2002 which served as the input and output reference images respectively. Bands 2, 4 and 5 were used to create the composite image for 1992 (see Figure 7) to minimize cloud cover along the coastal area. Bands 2, 4 and 5 were used to create the composite image for 2002 (see Figure 8).

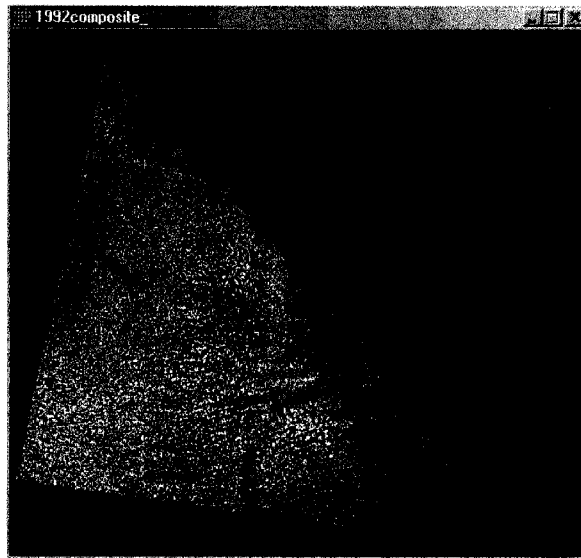


Figure 7: Composite Image for 1992



Figure 8: Composite Image for 2002

Metadata for both image files were created when the image bands were initially imported to Idrisi. The reference parameters consisted of the number of rows and

columns, the maximum and minimum values of X and Y, the reference system used, the reference units used and the unit distance (see Figure 9).

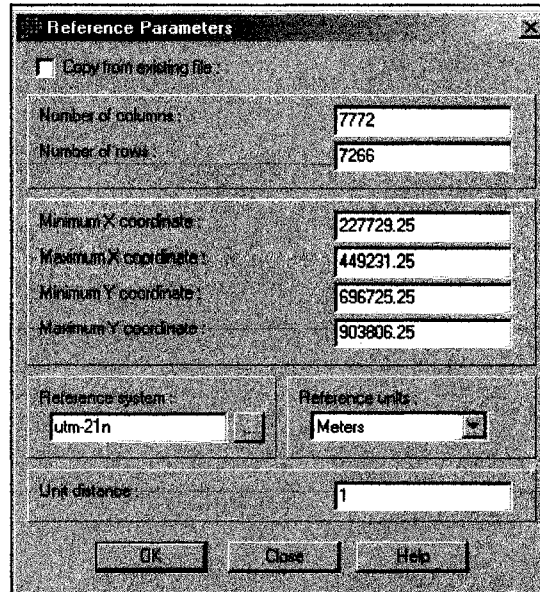


Figure 9: Reference Parameters Window Used in the Resample Module Showing the Parameters Copied from Band 2 of the 1992 Image.

The composite images for 1992 and 2002 were displayed as the Input reference and Output reference, respectively. The selected Mapping function was Linear, and Bilinear was chosen as the Resampling type (see Figure 10).

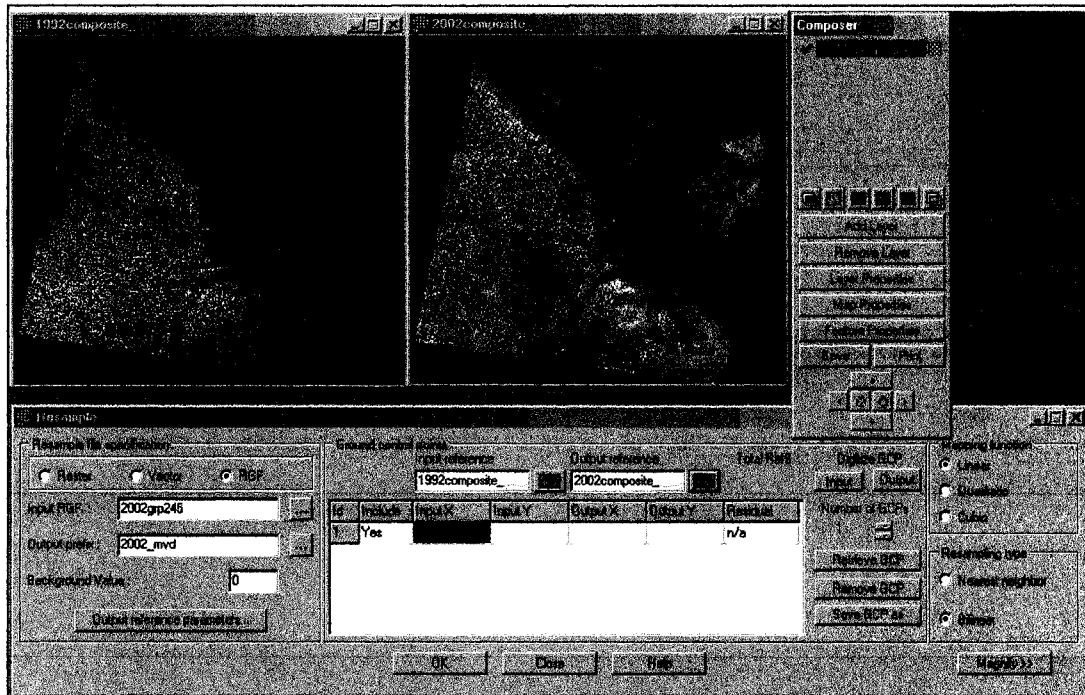


Figure 10: Resample Window Showing Two Composite Images for 1992 and 2002

The ground control points are input sequentially. The first ground control point (GCP) is located in Georgetown near the Demerara River. The first GCP is shown in Figure 11.

An additional three ground control points are added to the reference images.

Figure 12 shows the Total RMS for the first four GCPs. The Total RMS appears after the input of the fourth GCP. The Residual amounts associated with each GCP (see Figure 12) describe how far the individual GCPs deviate from the best fit equation (calculated using the four GCPs). It can be seen from Figure 12 that GCP 2, with a value of approximately 168, deviates the most from the best fit equation.

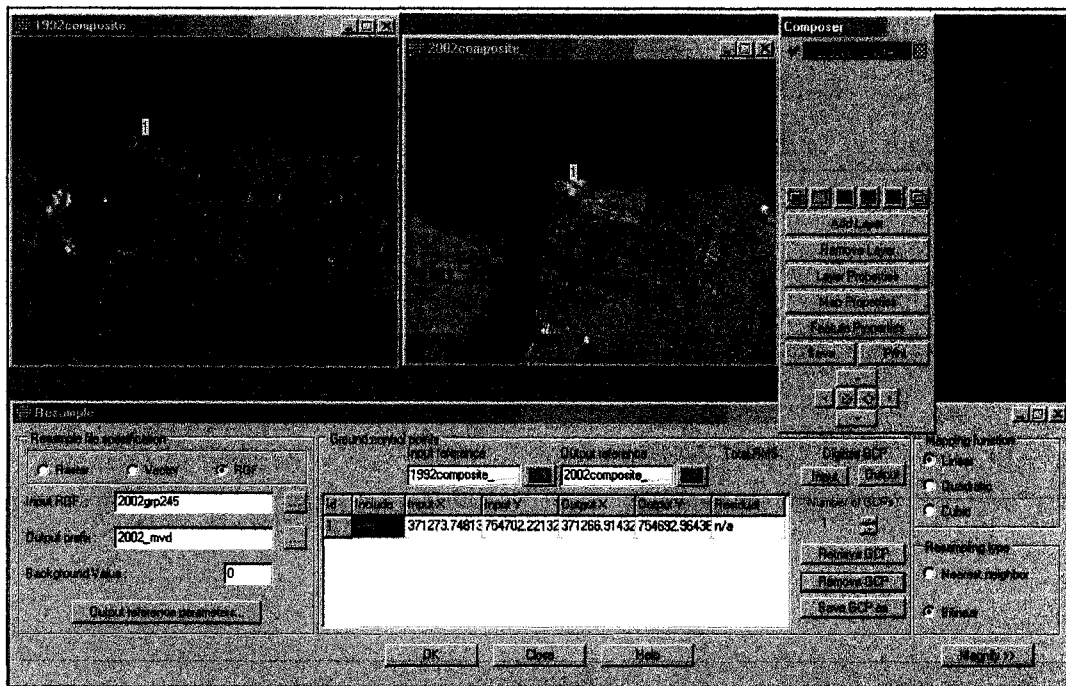


Figure 11: First Ground Control Point Shown in the Input and Output Reference Images

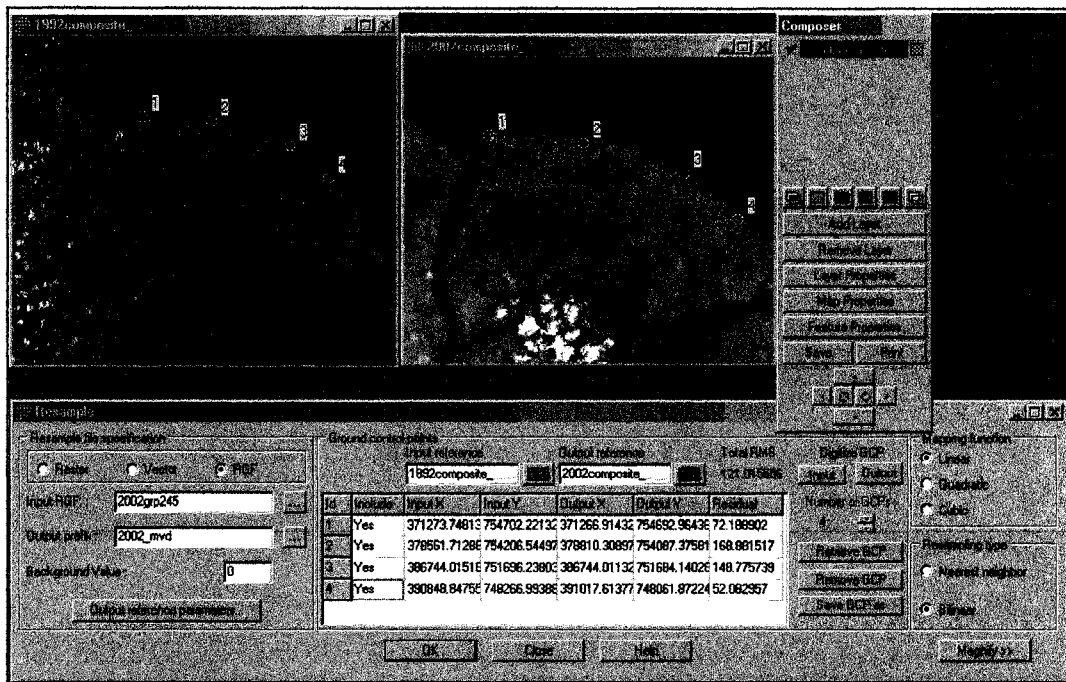


Figure 12: Four Ground Control Points Showing the Total RMS Error

At this stage of GCP input the Total RMS is 121.015. This value describes the overall positional error of the four GCPs in relation to the best fit equation, or the probability that a mapped position varies from its true location (see Clark Labs, 2003). According to US mapping standards, an acceptable Total RMS for images should be less than one-half of the resolution of the input image. In the case of Landsat images which have resolution of 30 m, an acceptable Total RMS would be 15 m. It can be seen from Figure 12 that the current Total RMS is approximately 121 m. At this stage, the four GCPs can be repositioned in one or both of the reference images to reduce the Residual values and therefore the Total RMS. GCP 2 would be the first candidate for repositioning due to the high associated Residual value. The objective in inputting the remaining GCPs will be to reduce the Total RMS to below 15 m.

A further 21 ground control points are input for a total of 25 ground control points. The accuracy of the position can be determined as the GCP is added. The Total RMS is updated with the input of each additional GCP. When all 25 GCPs have been input, various GCPs with large Residuals can be targeted for repositioning. When the Total RMS is at an acceptable level (less than 15 m), the input of GCPs is considered complete. GCPs can be saved for later retrieval; individual GCPs can be removed, or specified as Omitted so that they are not included in the calculation of the Total RMS. Figure 13 shows the Resample window with GCPs on the Input and Output reference images, and the Total RMS. A Total RMS of 6.75 m is considered acceptable.

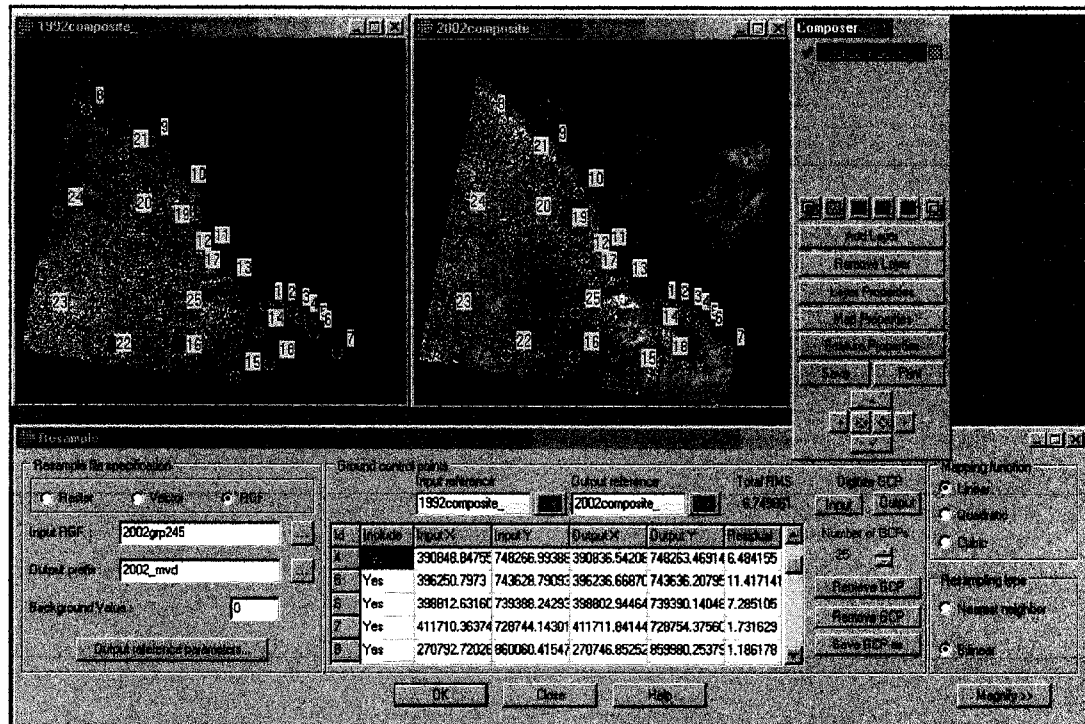


Figure 13: Resample Window Showing GCPs on Both Reference Images. The Total RMS is 6.75 m.

The Resample module is initiated with the current set of GCPs by clicking on the OK button. When complete, three new image files are created for Bands 2, 4 and 5 for the 2002 image. Each image band has the prefix “2002_mvd” attached to its name.

3.3.2 Project all the Image Bands for 1992 and 2002 to UTM-21N

Even though the specified coordinate system is UTM Zone 21N for both the 1992 and 2002 image bands, the Project module was used on all the image bands to remove any potential anomalies or distortions that may exist in the data set due to the resampling

process. Project can also be used to change the resolution of an image by a non-integer multiple by specifying the same output reference system as the current input reference system.

The type of file to be projected was raster. The input file and input reference system together with the output filename and reference file for output result were specified. The Resample type was Bilinear and the background value was left at 0.

For the 1992 image bands all files were projected to the Band 2, 1992 image which was used as the reference image. For the 2002 image bands all files were projected to the Band 2, 2002 image which was used as the reference image. Each output filename included the short form “proj” (for example, 1992_b2_proj) to indicate that these image files would be used in further processing. After resampling and projection, the image resolution for the image bands for 1992 and 2002 was 28.5 m

3.3.3 Creation of Mask File for the Background

A sample Landsat Image is shown in Figure 14. Note that the image has a black background. Normally, this background is omitted from image processing. A mask file can be used to mask out the surrounding black background box. The Reclass module can be used to create a mask image file.

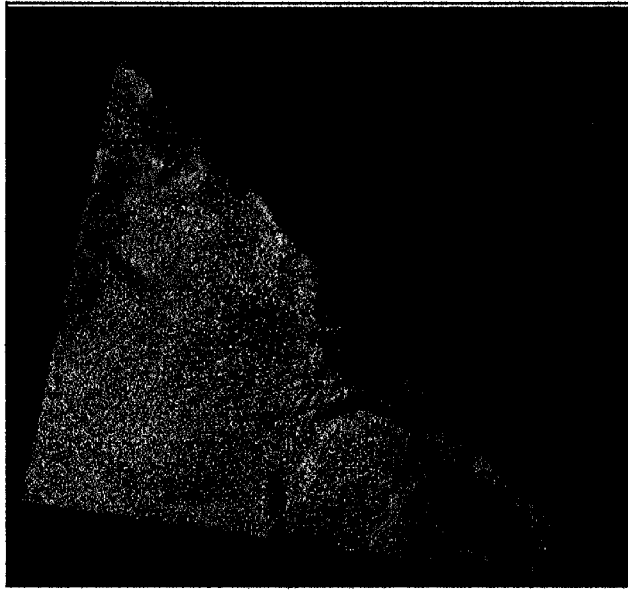


Figure 14: Sample Landsat Image for the Study Area

Creating Image Mask File to Mask Out Background Values of 0 (i.e., black)

The Reclass module is available from the GIS Analysis, Database Query menu. The Reclass module was used as follows.

1. The type of file to reclass was specified as image.
2. The classification type was user-defined reclass.
3. The input file in this case was a previously geometrically corrected image file for Landsat 5 TM Band 2, 1992.
4. The output file was named: Mask_for_Background.rst

5. The reclass parameters were as follows:

<u>Assign a new value of</u>	<u>To all values from</u>	<u>To just less than</u>
0	-1	1
1	1	256

The Reclass window is shown in Figure 15.

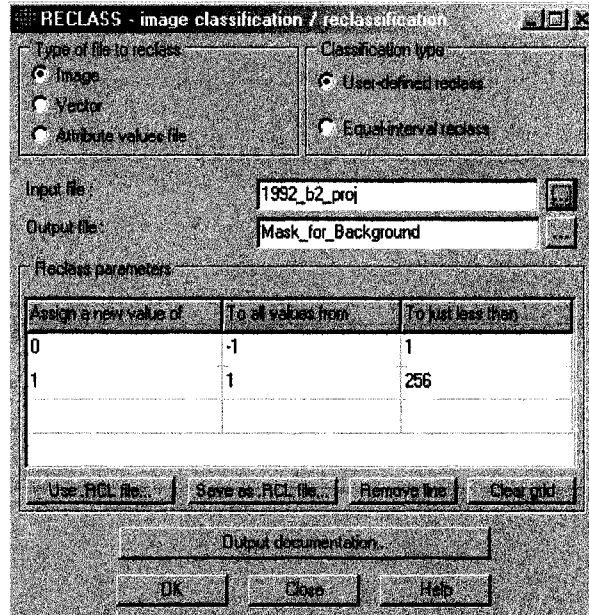


Figure 15 Reclass Window Showing the Reclassification Values for the Mask File

The resulting Mask_for_Background file is shown in Figure 16.



Figure 16: Mask Image for Background (0 = Black, the background) 1 = Red

The Project module was used to project the Mask_for_Background file to the UTM-21N coordinate system. The reference file for output result is given as UTM-21N. Resample type is given as Bilinear. The Background value is 0. The output reference information button opens a new window called Reference Parameters. This window requires the number of rows and columns in the image together with the Maximum and Minimum X, Y coordinates. The option to copy the reference parameters from an existing file is used. In this case, the previously geometrically corrected image for Landsat 5 TM Band 2, 1992 was used. After clicking on the OK button in the PROJECT window, the operation is completed. The file Mask_for_Back_Proj will be specified with any module where the background polygon is to be excluded in processing. This is specified as

Mask_for_Back_Proj.

3.4 Description of General Methodology and Principles

Since one of the objectives of this study is to detect positional change of the coastline between 1992 and 2002 it is necessary to extract the coastline from both the 1992 image and the 2002 image. Composite images could be created and exported to ArcMap for manual digitizing of the coastline, but this would be tedious and time consuming. From the literature it is known that several techniques have been advocated for automatically extracting a coastline from a remote sensing image. After evaluating various automatic extraction techniques presented in the literature the decision was made to utilize the procedure proposed by Alesheikh *et al.* (2004). Figure 17 presents a flowchart of the technique for extracting coastlines from remotely sensed images.

For each of the two image years, bands 2, 4 and 5 will be utilized. Band 2 represents the green strip (0.52-0.60 μm) of the visible end of the electromagnetic spectrum where the reflectance of water is maximized. Additionally, band 2 serves to act as a measure of 'greenness' for vegetation and its corresponding characteristic of high reflectance. Bands 4 and 5 represent the near infrared (0.75-0.90 μm) and mid infrared (1.55-1.75 μm) band widths respectively. Both bands 4 and 5 are characteristic of low reflectivity of water and high reflectivity of vegetation and soil. Band 5 is used because it is usually the best spectral band for discriminating the interface between water and land. In particular, the mid-infrared spectral environment of water found within band 5 is characterized by very low reflectance due to the high absorption of electromagnetic

energy by a water body including turbid water (Alesheikh *et al.*, 2004). As a result, the corresponding average radiant flux values received by the TM and ETM+ sensors

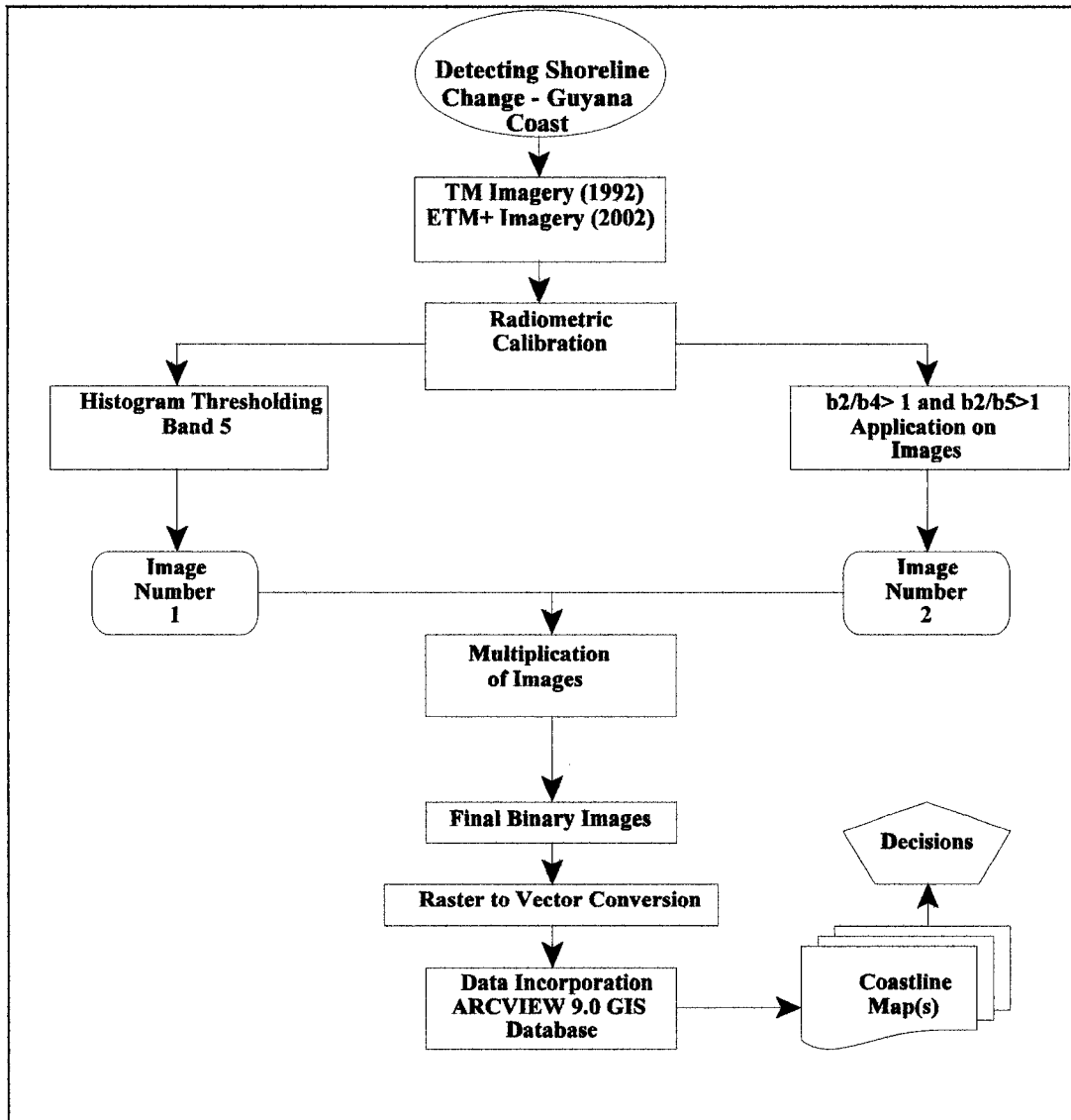


Figure 17: Flowchart design of coastline extraction technique for remote sensing images as proposed by Alesheikh *et al.* 2004.

expressed as digital numbers (DNs) would register as zero or values approaching zero. Conversely, band 5 shows high reflectance for both vegetation and soil resulting in corresponding radiance values expressed as high DN's. The strong contrast between water and land values allows for the delineation of the interface between these two mediums and will ultimately help to determine shoreline position.

3.4.1 Radiometric Correction - An Overview

In order to provide an image that resembles an accurate representation of the earth's surface it is necessary to remove or reduce distortions encountered in the image acquisition process (Lillesand et. al., 2004). According to Sabins (1987), the source of any distortion is the result of systematic (satellite and sensor induced) or non-systematic (environment and atmospheric induced) errors. Systematic errors and distortion are associated with data transmission problems, satellite orbit and path and anomalies referred to as random 'noise'. Among common systematic errors, image banding or striping caused by satellite sensors out of calibration and scan line drop out due to signal loss resulting in the omission of scan lines of data cause image distortion.

Similarly, non-systematic errors associated with environmental and atmospheric conditions may effect the path radiance from the sensor to ground object and vice versa. For example, earth-sun distance and sun elevation corrections are necessary when comparing images of different locations and times in order to normalize average pixel brightness values given the varied solar elevation angle throughout the seasons (Lillesand et al., 2004). In addition, topographic attenuation caused by slope and aspect of certain

ground features may vary the illumination levels within a scene by casting shadows on adjacent similar features resulting in false radiant values (Jensen, 1996). Further atmospheric effects include the scattering and absorption of radiant energy by atmospheric particles (ie. water vapour, particulant matter) which encourages a reduction in path radiance upon a ground object or increases path radiance via reflection back through the satellite sensors. The former effect will reduce illumination upon a ground object and result in lower average radiant values expressed as DNs, the latter effect will elevate radiant measures of illumination expressed as higher than expected DNs. In both cases, atmospheric effects will falsify the expected radiant values and negatively skew the ensuing ground image.

In the analysis, each of the six spectral bands will be radiometrically corrected using Idrisi's Radiance module. Two initial images (Image 1 and Image 2) would be produced, one for 1992 and one for 2002 - (see Radiometric Correction).

3.4.2 Band Ratioing

In processing the two images, band ratioing was used because ratio images emphasize differences in slopes of spectral reflectance curves between the two bands of the ratio. Individual ratio images allow for the extraction of reflectance variations (Sabins, 1987). For each of the two years, two band ratios were developed; namely, Band 2/Band 4 and Band 2/Band 5. From the literature (McFeeters, 1996), band ratioing of Bands 2 and 4 is known to enhance the differences in pixel resolution between water

and land based on the fact that the typical reflectance of water is maximized in the visible band of the electromagnetic spectrum (TM and ETM+ Band 2) and minimized within the near-infrared (TM and ETM+ Band 4) and mid-infrared (TM and ETM+ band 5) respectively. Conversely, Bands 4 and 5 display high reflectance of land based cover such as soil and vegetation within the near and mid-infrared electromagnetic spectrum found in Bands 4 and 5. In the analysis, the ratios generated between Band 2/Band 4 and Band 2/Band 5 were either greater than one denoting water or less than one denoting land. The resultant binary classification was used to delineate the water-land interface and an intermediate image referred to as Image 2 was generated for both years.

3.4.3 Histogram Thresholding

For each year, histogram thresholding was done using Band 5. The selection of Band 5 has proven to be a good indicator of the spectral differences between land and water based on its aforementioned spectral characteristics. When examining a histogram of a scene contained within the coastal zone, the bimodal presentation reveals a sharp peak skewed to the left of the histogram, another peak skewed to the right and a trough that separates the two (see Figure 18). The former distribution reveals the presence of water as noted by DNs approaching zero or near zero levels. The latter distribution depicts the presence of land values (soil and/or vegetation) as noted by higher brightness values. The trough found within the histogram separating these two distinct zones is the interface between land and water. Values expressed as DNs found to the left of this interface (trough) would represent water pixels, conversely values found to the right of

the trough would be classified as land pixels. Ultimately, this information will help to ascertain the coastline position during binary classification.

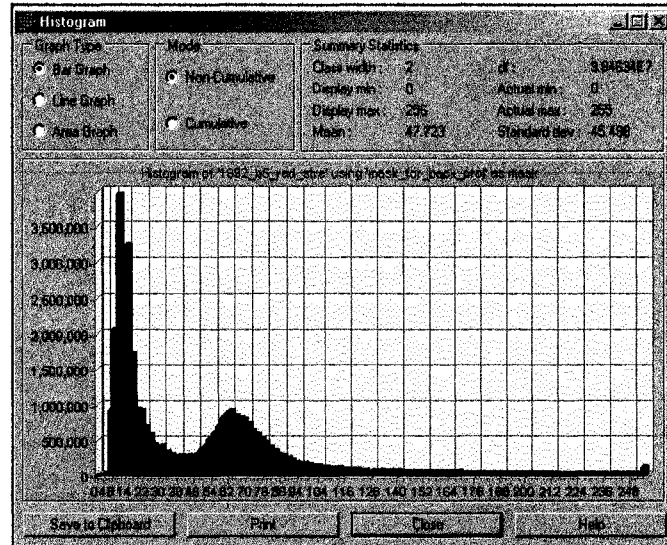


Figure 18: Sample Histogram Showing Two Peaks

The resulting images were binary images with land classified as 0 and water classified as 1. These images were designated as Image 1 for each year. For each year, Image 2 was derived from two intermediate images generated through the band ratioing process. For each year, Image 1 was multiplied by Image 2 to obtain the final binary image for each year. The two final binary images showed a fairly good delineation between land and water. This final binary images were exported from Idrisi to ArcGIS as GeoTiff files. The ArcGIS extension, ArcScan, was used to aid in converting the raster images to vector files.

A geometrically corrected and rectified composite image for each year was produced in Idrisi and exported as a GeoTiff image. For each year the composite images

were used in ArcGIS to assess the accuracy of the coastline vector files obtained using ArcScan. Any necessary adjustments to the coastline was made using the Editing tools available in ArcMap. After radiometric calibration for each image band, two initial images were produced for each year (1992 and 2002). For the year 1992, the initial image was the result of histogram thresholding on Band 5 so that the resulting image had land classified as 0 and water classified as 1. The initial image was designated as Image 1. The second image was produced by using a logical AND operation on two intermediate band ratioed images. The first intermediate image was Band 2/Band 4 reclassified so that land = 0 and water = 1. The second intermediate image was Band 2/Band 5 reclassified so that land = 0 and water = 1. The logical AND operation on the two intermediate images produced the second image. The second image was designated as Image 2.

Image 1 and Image 2 were multiplied together to obtain a final binary image. The final binary image revealed a fairly good delineation between land and water. A composite map for both image years, 1992 and 2002, was exported from Idrisi as a GeoTiff file so that the images could be imported to ArcMap. The raster files were used to compare the vector files showing the shorelines to ascertain whether any corrections were required to the generated coastlines for each year.

3.4.4 GIS Input and Analysis

The outputs from image processing were exported for input into the ARCVIEW GIS database (ESRI, 2001). A spatially referenced GIS database will be able to show the temporal variations and spatial extents of coastline changes in the near and offshore zones of Guyana. One of the unique aspects of the GIS system is that it produced maps to show how the coastline varied along different sections of the coast for both time periods.

4.0 ANALYSIS

4.1 Radiometric Correction

The Idrisi module, Radiance, converts raw satellite DN values to calibrated radiances using lookup tables of gain and offset setting for LANDSAT satellites 1-5, and user-defined values for Lmin/Lmax or Offset/Gain for other sensor systems. Conversion to radiances was used to facilitate comparisons between images from different dates.

Radiometric correction was performed since two different sensors are used for two different years, namely 1992 and 2002. The 1992 image is a Landsat 4 Thematic Mapper image and the 2002 image is a Landsat 7 Enhanced Thematic Mapper Plus image.

4.1.1 1992 Image

Figure 19 shows the Radiance window used to convert the digital numbers (DN) in Band 2, 1992 to radiance values. It can be seen in Figure 19 that for Landsat 1-5, the Landsat - 4/5 TM (TIPS-ERA after Jan 15, 1984) was selected. Note that Band number 2 was specified. It is worthwhile to note that the resulting file, given the name "1992_b2_rad" has the data type as "real". The range of values extend from a minimum of -28.8 to a maximum of 29.5621. Some Idrisi modules cannot be utilized on files with data type as "real". Therefore, the Stretch module was used to stretch the values from 0 to 255. This operation changed the data type to byte. The resulting image file is shown in Figure 20.

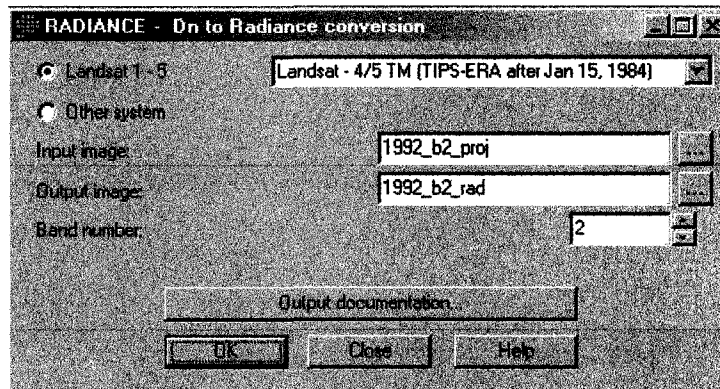


Figure 19: Band 2, 1992: Convert DN Values to Radiance

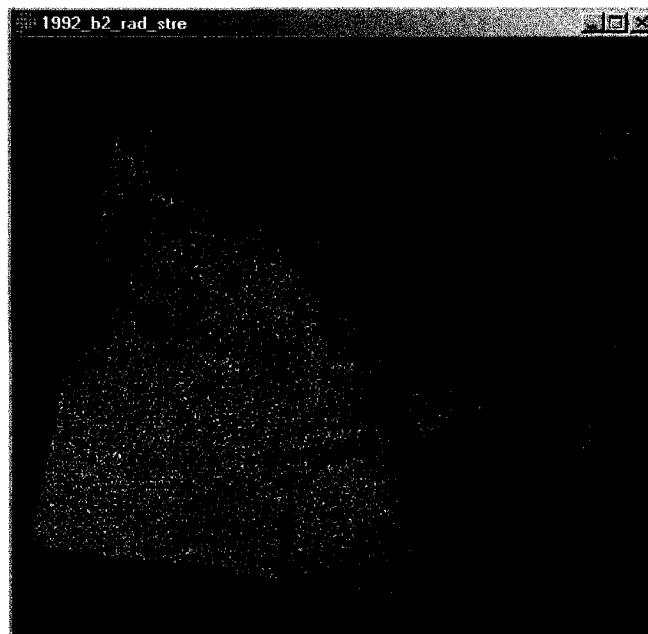


Figure 20: Band 2, 1992 After Using Radiance Module and Stretch Module

Based on the outlined methodology, only Bands 2, 4 and 5 were used for each image year. Therefore, the Radiance module was used on the remaining image bands. The Stretch module was used so that the DN values range from 0 to 255 which provided good contrast, and also changed the data type from real to byte.

4.1.2 2002 Image

Figure 21 shows the Radiance window used to convert the digital numbers (DN) in Band 2, 2002 to radiance values. It can be seen in Figure 21 that for Landsat 7 ETM+, Other system was specified. This was because the version of the software did not include

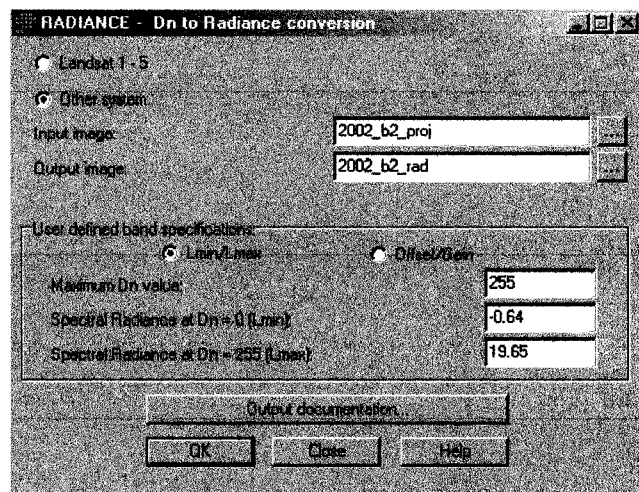


Figure 21: Band 2, 2002: Convert DN Values to Radiance

lookup tables for the Landsat 7 sensor. Therefore, three user defined band specifications had to be specified. These were maximum DN value, spectral radiance at DN = 0 (Lmin), and spectral radiance at DN = 255 (Lmax). In addition, either Lmin/Lmax or Offset/Gain had to be selected.

The information required for the 2002 image was obtained from two sources. The calibration for ETM+ sensor spectral range values for low and high gain mode for each band were obtained from a Landsat frequently asked question document from the US

Table 3 - ETM+-7 spectral range values in low gain mode.

Band	1	2	3	4	5	6	7	8
Lmin (W/m ² *sr*μ)	-6,2	-6,4	-5	-5,1	-1	0	-0,35	-4,7
Lmax (W/m ² *sr*μ)	293,7	300,9	234,4	241,1	47,57	17,04	16,54	243,1
Offset = Lmin, (A0)	-6,2	-6,4	-5	-5,1	-1	0	-0,35	-4,7
Gain = (Lmax-Lmin)/255, (A1)	1,1761	1,2051	0,9388	0,9655	0,1905	0,0668	0,0662	0,9718

Table 4 - ETM+-7 spectral range values in high gain mode.

Band	1	2	3	4	5	6	7	8
Lmin (W/m ² *sr*μ)	-6,2	-6,4	-5	-5,1	-1	3,2	-0,35	-4,7
Lmax (W/m ² *sr*μ)	191,6	196,5	152,9	157,4	31,06	12,65	10,8	158,3
Offset = Lmin, (A0)	-6,2	-6,4	-5	-5,1	-1	3,2	-0,35	-4,7
Gain = (Lmax-Lmin)/255, (A1)	0,7757	0,7957	0,6192	0,6373	0,1257	0,0371	0,0437	0,6392

Source: European Space Agency, 2006. Landsat Frequently Asked Questions. Earth Observation Quality Control. Earthnet Online. Earth Observation. As of September 20, 2006.

Geological Survey and posted on the European Space Agency web site. This information is shown in Tables 3 and 4. The gain mode for each band on October 1, 2002 was included with the metadata supplied with the image. Using this information it was possible to provide the appropriate information in the Radiance window.

The metadata for October 1, 2002 indicated that Band 2 was taken in high gain mode. Using Table 4, the Lmin value was determined to be -0.64 (-6.4 / 10), and the Lmax value was determined to be 19.65 (196.5 / 10). The maximum DN value in Band 2 was 255. Clicking on the OK button produced the radiance image. As done for the 1992 image bands, the Stretch module was used so that the DN values stretched from 0 to 255 so that the image bands can be used in other Idrisi modules.

The resulting image for Band 2, 2002 is shown in Figure 22. Band 4, 2002 was taken in low gain mode and the values found in Table 3 were used to input the Lmin and Lmax values in the Radiance window. Similarly, Band 5, 2002 was taken in high gain mode and the values found in Table 4 were used to input the Lmin and Lmax values.



Figure 22: Band 2, 2002 After Using Radiance Module and Stretch Module

4.2 Image Processing According to Methodological Principles

4.2.1 Obtaining Image 1 for 1992

Band 5, 1992

Band 5 is frequently used because it was found to be best, in most instances, for distinguishing the interface between land and water (Alesheikh *et al.*, 2004, Ouma and Tateishi, 2006). Band 5 is in the mid-infrared range (1.55-1.75 μm), and water exhibits a high degree of absorption of the energy in this spectral band while vegetation has strong reflectance in this spectral band (Alesheikh *et al.*, 2004, Ouma and Tateishi, 2006).

After radiometrically correcting Band 5, 1992 it was stretched to show DN values of 0-255. The background polygon has a value of 0. The data type is byte. The filename is currently 1992_b5_rad_stre. This image is shown in Figure 23. It can be seen in Figure 23

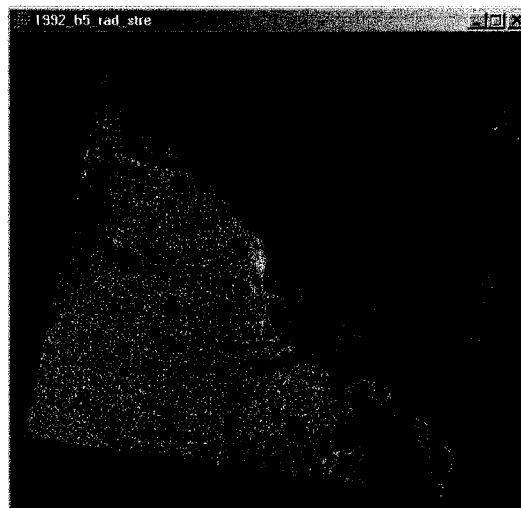


Figure 23: Band 5, 1992 After Using Radiance Module and Stretch Module

that land and water areas appear quite distinct except where there is cloud.

Histogram thresholding was done in order to create a binary image that separates land from water. The Histo module in Idrisi was used. A histogram using the module's default values was produced and is shown in Figure 24. The histogram in Figure 24 shows two peaks. The lower DN values represent water, the higher DN values represent land. For the histogram in Figure 24, 38 was determined to best demarcate land from water.

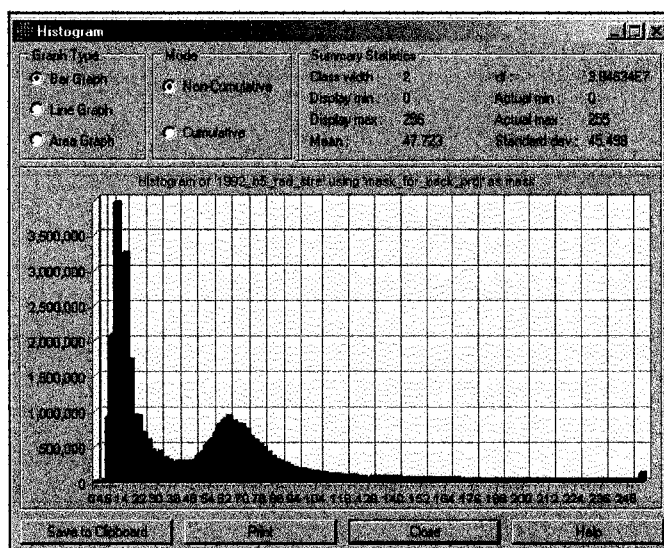


Figure 24: Histogram for 1992_b5_rad_stre Showing Two Peaks

The Reclass module was then used to reclassify the image file. The reclass parameters were specified as follows:

<u>Assign a new value of</u>	<u>To all values from</u>	<u>To just less than</u>
-5	-0.001	0.001
1	0.001	39
0	39	256

After reclassification, the image band was named 1992_b5_rad_stre_3classes_image1. This image is shown in Figure 25. The image represents the land-water boundary using thresholding on Band 5. It should be noted that the selection of the threshold value is based on the information provided by the histogram and is not exact. Some pixels that are water may be classified as land and vice versa. It can be seen in Figure 25 that there is visible haze over areas of water that extend onto land, and the offshore coastal area is known to carry sediments. Turbid areas offshore could be incorrectly classified as land whereas the area may actually be sediment-laden water.

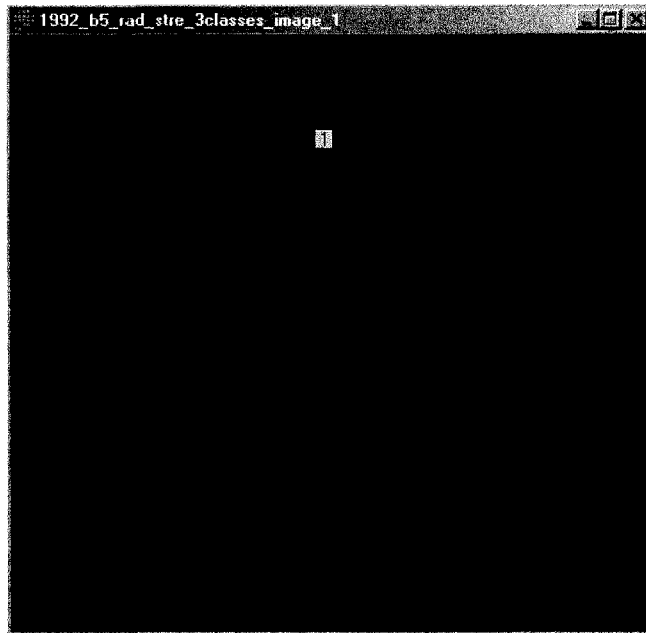


Figure 25: Reclassified Image
1992_b5_rad_stre_3classes_Image1 Showing
Land/Water Boundary. Note problematic cloud areas
near the coast

4.2.2 Obtaining Image 1 for 2002

Band 5, 2002

Band 5 for the year 2002 is shown in Figure 26. Finding DN values that would indicate a boundary between land and water required the use of Idrisi's Update module. The Input image name was specified. The input requirement for the module is the Value

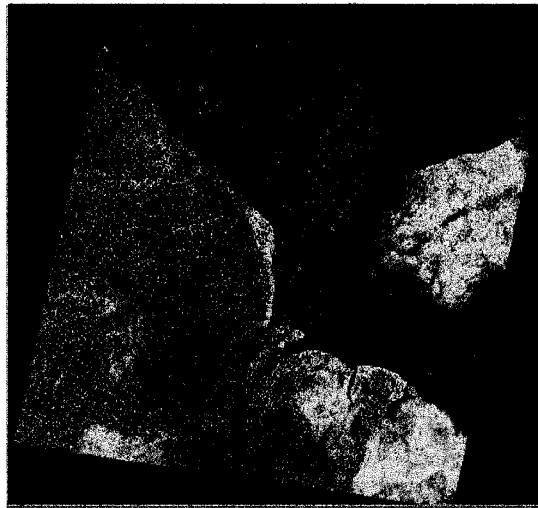


Figure 26: Band 5, 2002

to be given to the First row, Last row, First column, and Last column. This assigns a new value to the pixels within the designated row/column area. The Update module was run several times to avoid assigning water values to the background polygon. The updated image is shown in Figure 27.

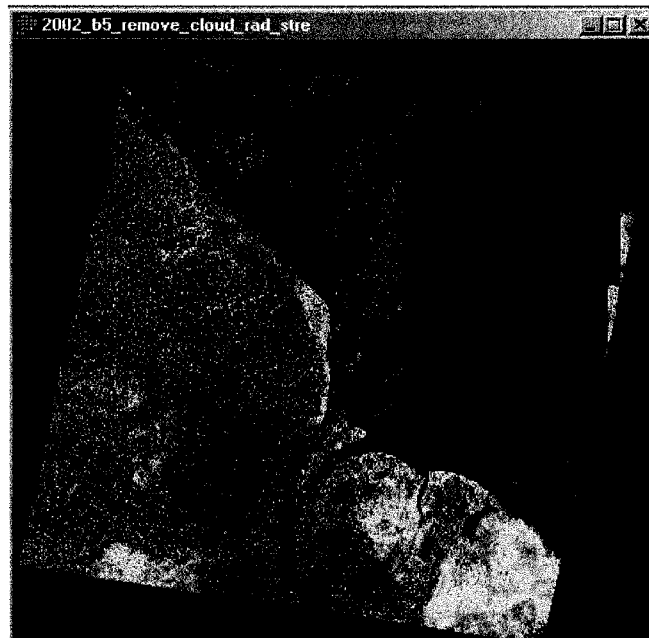


Figure 27: Band 5, 2002 Showing the Major Cloud Area Updated With the Values of Water Pixels.

The Histo module is used to display a histogram using the default values. The histogram is shown in Figure 28. In this case, the Histo module was run again, this time using the

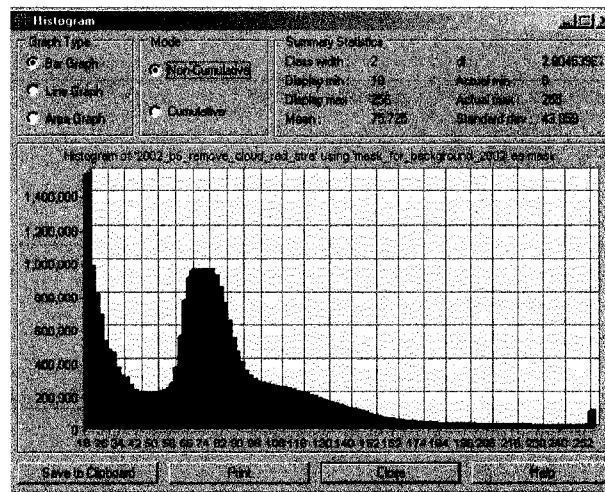


Figure 28: Histogram for 2002_b5_remove_cloud_rad_stre Showing 2 Peaks

Output type of Numeric to gain a better understanding of the histogram distribution.

Together with Cursor Inquiry mode, it was determined that the best approximate value to delineate water from land was 47.

The reclassified image for Band 5, 2002 is shown in Figure 29.



Figure 29: Reclassified Image for Band 5, 2002 Showing the Land/Water Boundary.

4.2.3 Obtaining Image 2 for 1992

Band Ratioing

Band ratioing was done using Bands 2, 4 and 5 for 1992. Band 2, 1992 can be seen in Figure 20. Band 5, 1992 can be seen in Figure 23. Band 4, 1992 is shown in Figure 30.

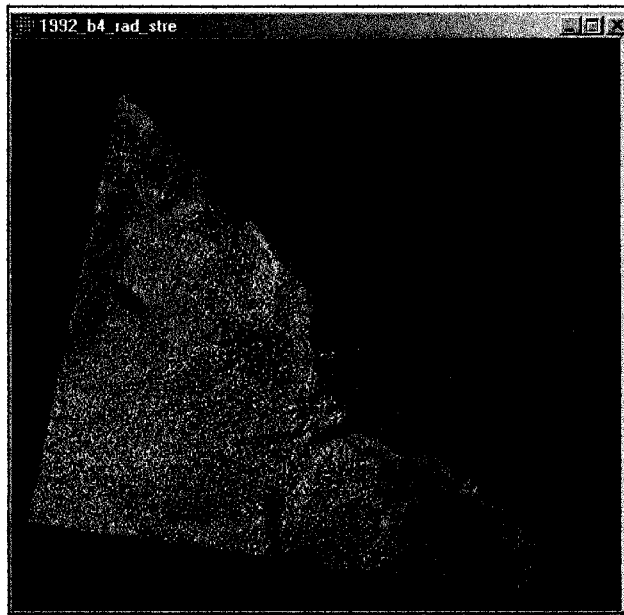


Figure 30: Band 4,1992 (1992_b4_rad_stre)

Using the Overlay module (see Figure 31) from the GIS Analysis, Database Query menu, Band 2 is divided by Band 4 to produce a ratioed image (First/Second in the Overlay window). In the Overlay window, Division by zero is specified as resulting in the value 0 instead of an error.

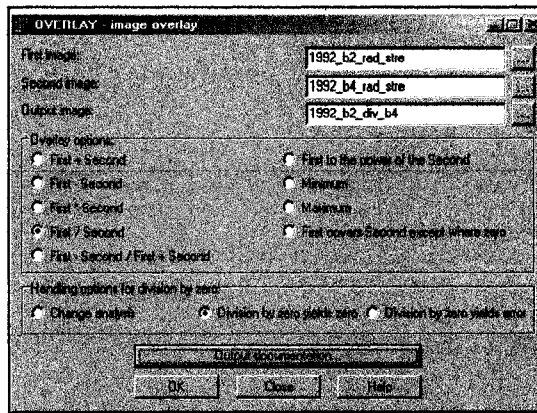


Figure 31: Overlay Window for Band 2 / Band 4 for 1992

The resulting image file has a data type of “real”. The resulting filename is 1992_b2_div_b4 and is shown in Figure 32.

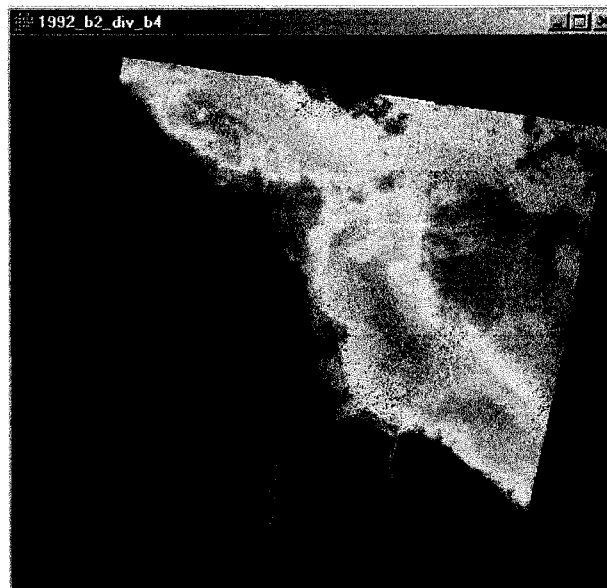


Figure 32: 1992_b2_div_b4

A similar procedure is used to produce the ratio image for Band 2 divided by Band 5. The resulting filename is 1992_b2_div_b5 and the image is shown in Figure 33.

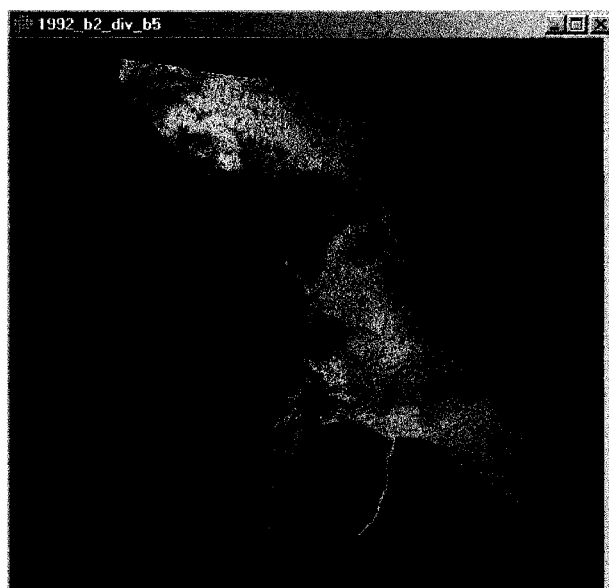


Figure 33: 1992_b2_div_b5

The histogram for Band 2/Band 4, 1992 is shown in Figure 34. The histogram for Band 2/Band 5 is shown in Figure 35. It can be seen from the histograms in Figures 34

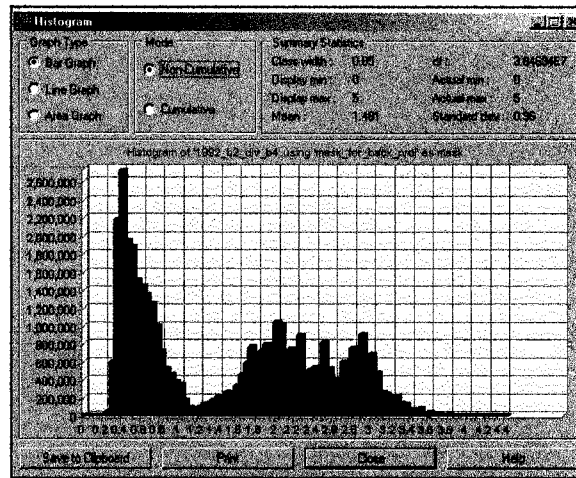


Figure 34: Histogram for 1992 Band 2/Band 4

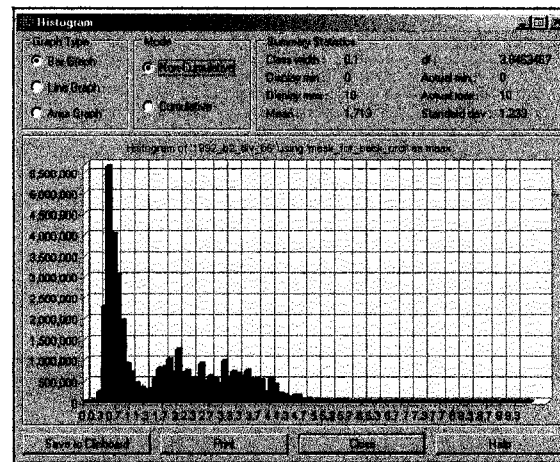


Figure 35: Histogram for 1992 Band 2/Band 5

and 35 that the maximum value in Figure 34 is 5 and the maximum value for Figure 35 is 10. The values contain decimal points, indicative of the data type “real”. It can be noted that the break between the two “peaks” in each histogram occurs at the approximate value

of 1. Hence, creating an image where the ratio is greater than 1 would create an image where the water area is classed as "1" and everything else is classed as "0". To do this the Image Calculator is used. For Band 2 / Band 4 the output filename will be 1992_b2_div_b4_gt_1. The Expression to process is: $1992_b2_div_b4 > 1$. Figure 36 shows the Image Calculator window with the abovementioned expression.

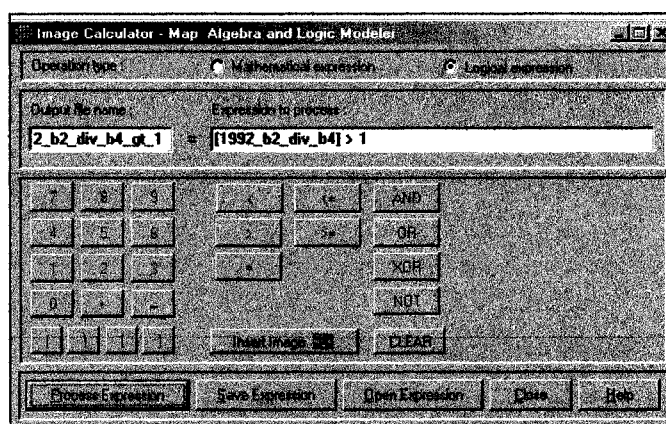


Figure 36: Image Calculator Window to Evaluate the Expression: $1992_b2_div_b4 > 1$

Figures 37 and 38 show the resulting images: $b2/b4 > 1$ and $b2/b5 > 1$. The land area and background are coded with the value "0". The water area is coded with the value of "1". The data type for these image files is byte binary.

Performing a logical AND using these two images (Figures 37 and 38) should find the common coastline area. The Image Calculator is used again, and the resulting file is shown in Figure 39.

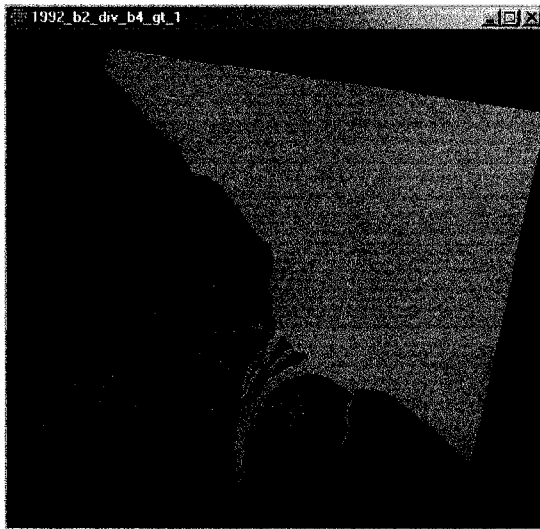


Figure 37: Band 2 / Band 4 > 1

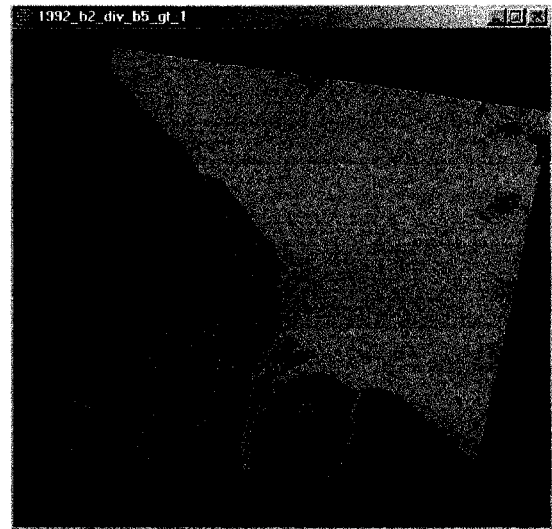


Figure 38: Band 2 / Band 5 > 1

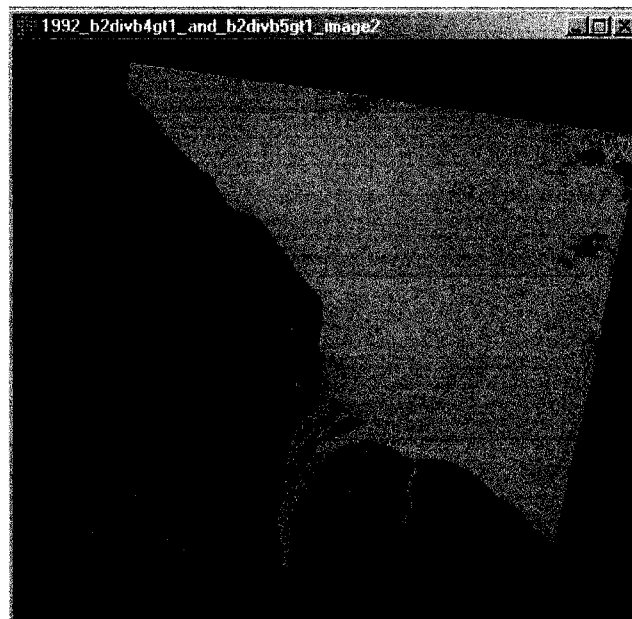


Figure 39: Image 2 Derived From (Band 2 / Band 4 > 1) AND (Band 2 / Band 5 > 1)

The background has been reclassified to 0, the same as land. When converting to vector, the background is to be ignored. Therefore, we will attempt to reclassify image 2 so that

the background can be separated from the land. The Reclass module is used to reclassify the image so that the background is coded -5, the land is coded 0 and the water is coded 1. The reclassified image is shown in Figure 40.



Figure 40: Reclassified Image 2 Where the background is coded -5, the land is coded 0, and the water is coded 1

4.2.4 Obtaining Image 2 for 2002

Band Ratioing

For 2002, band ratioing was also done using Bands 2, 4 and 5. Band 2, 2002 can be seen in Figure 41. Band 4, 2002 can be seen in Figure 42, and Band 5, 2002 can be seen in Figure 43.



Figure 41: Band 2, 2002 (2002_b2_rad_stre)



Figure 42: Band 4, 2002 (2002_b4_rad_stre)

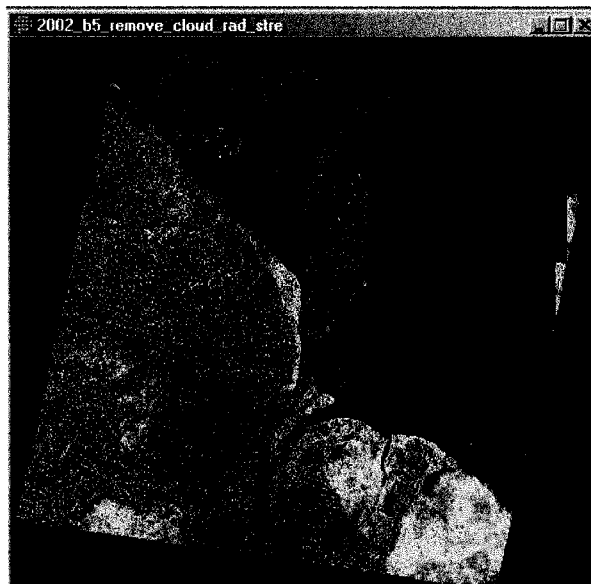


Figure 43: Band 5, 2002
(2002_b5_remove_cloud_rad_stre)

As before the Overlay module (see Figure 44) is used. Band 2 is divided by Band 4 to produce a ratioed image (First/Second in the Overlay window). The resulting image file has a data type of “real”. The resulting filename is 2002_b2_div_b4 and is shown in Figure 45. A similar procedure is used to produce the ratio image for Band 2 divided by

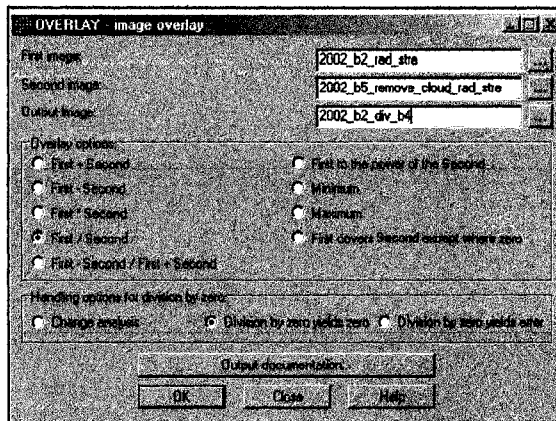


Figure 44: Overlay Window for Band 2 / Band 4 for 2002

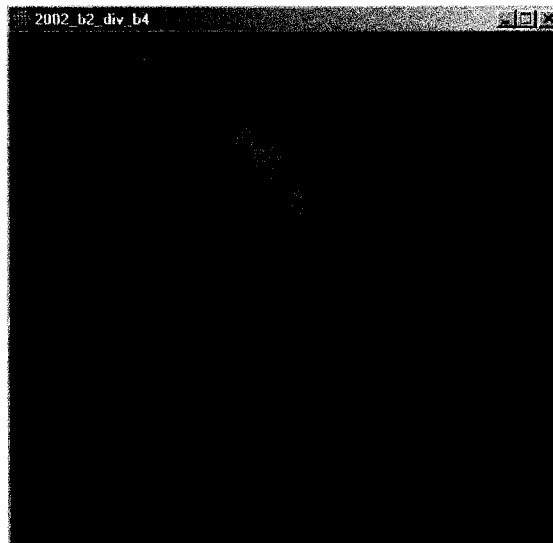


Figure 45: 2002_b2_div_b4

Band 5. The resulting filename is 2002_b2_div_b5_cldrmv and the image is shown in Figure 46.



Figure 46: 2002_b2_div_b5_cldrmv

The histogram for Band 2/Band 4, 2002 is shown in Figure 47.

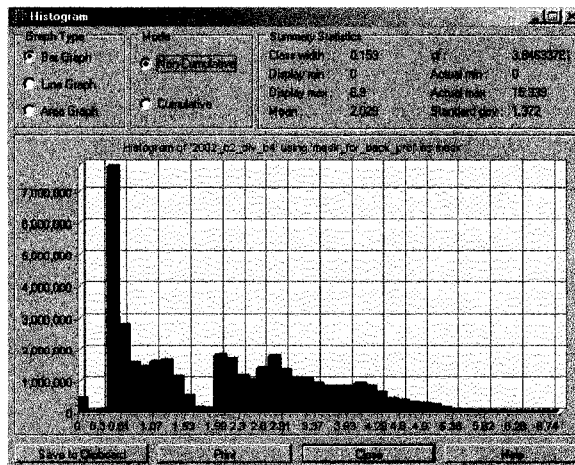


Figure 47: Histogram for 2002 Band 2/Band 4

The histogram for Band 2/Band 5 is shown in Figure 48.

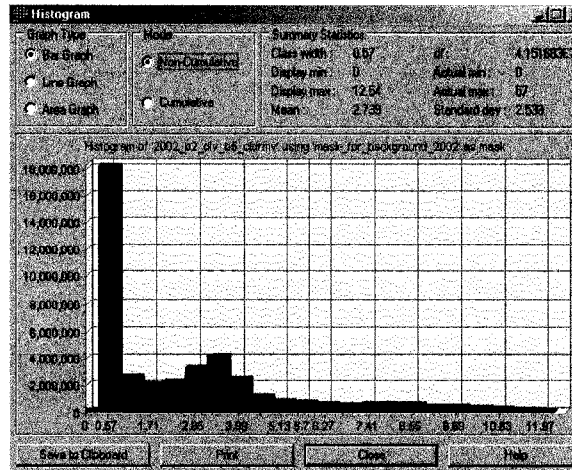


Figure 48: Histogram for 2002 Band 2/ Band 5

It can be seen in Figure 47 that the maximum value is 6.9. For Figure 48, the maximum value is 12.54. Both values contain decimal points, indicative of the data type “real”. In these two instances, there are two peaks in each histogram. It can be noted by using the Cursor Inquiry mode in Idrisi that the break between the two “peaks” in the histogram for Figure 47 occurs at the approximate value of 1.6. Hence, creating an image where the ratio is greater than 1.6 would create an image where the water area is classed as “1” and everything else is classed as “0”. To do this for Band 2/Band 4 the Image Calculator is used.

The Image Calculator (Figure 49) produced the image shown in Figure 50.

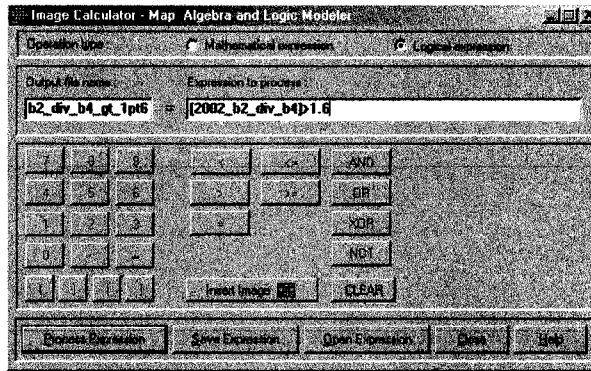


Figure 49: Image Calculator Window to Evaluate the Expression: 2002_b2_div_b4 > 1.6

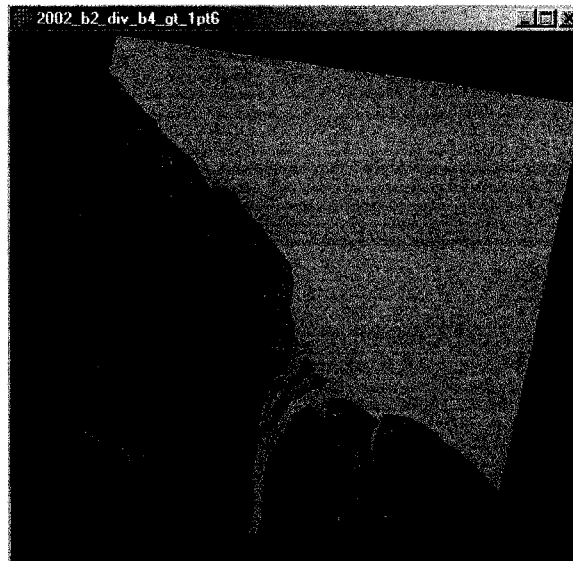


Figure 50: Band 2 / Band 4 > 1.6

The Image Calculator was used to produce an image with the filename:
 2002_b2_div_b5_cldrmv_gt_1pt25. This image is shown in Figure 51.

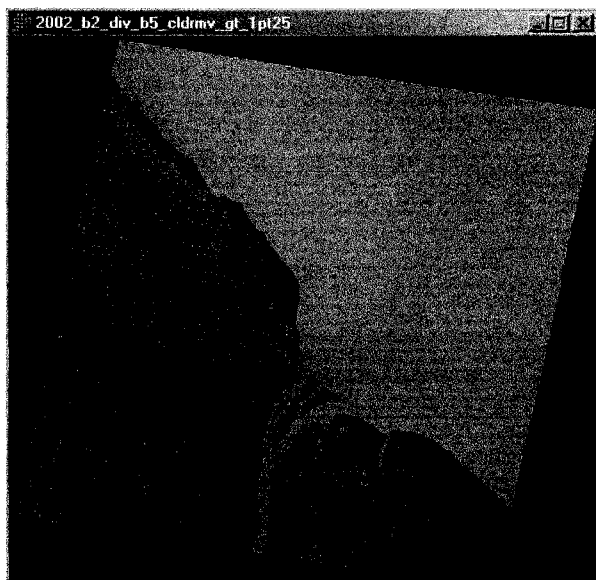


Figure 51: Band 2 / Band 5 > 1.25

Performing a logical AND using these two images should find the common coastline area. The resulting file is shown in Figure 52.

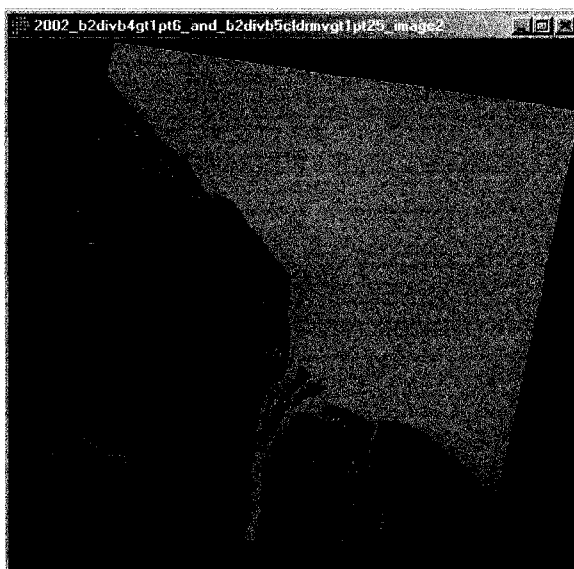


Figure 52: Image 2 Derived From (Band 2 / Band 4 > 1.6) AND (Band 2 / Band 5 > 1.25)

4.2.5 Multiplication of Image 1 and Image 2

1992

Image 1 (1992_b5_rad_stre_3classes_Image1) was multiplied by image 2 which was obtained using the logical AND operator on the two ratioed images (band 2/band 4 and band 2/band 5). The file was named 1992_image2_add1_times_mask_3classes_final. Both Images 1 and 2 have data type of integer. The multiplication of the two images was performed using the Overlay window. The result of multiplying images 1 and 2 is shown in Figure 53 (filename is 1992_image1_times_image2).



Figure 53: 1992 Image Derived from Multiplying Images 1 and 2

Before conversion to a vector file, it was decided to reclassify the image so that only three values occur. The background was reclassified to show a value of 0. Land was assigned a value of 1 and water a value of 10.

The resulting file (1992_final_binary_image_reclass; see Figure 54) has a data type of byte. The file was ready for conversion from a raster to a vector file.

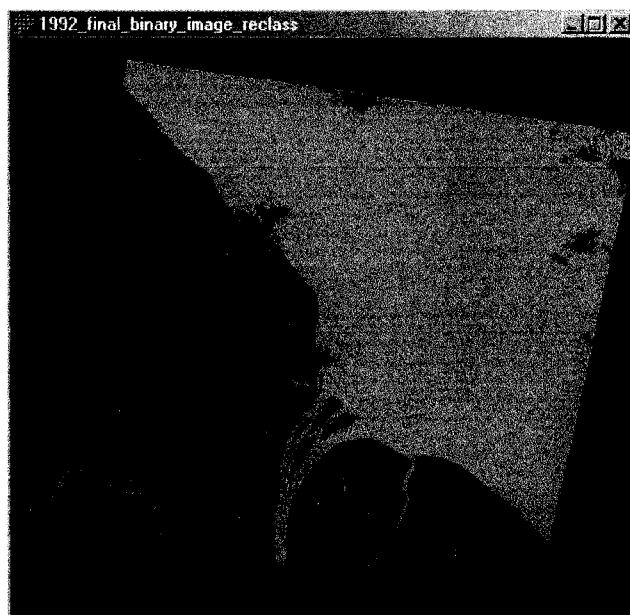


Figure 54: 1992 Final Image File Ready for Conversion to a Vector File

2002

The 2002 images were processed in the same manner as the images for 1992. Image 1 (2002_b5_remve_cld_rad_stre_3classes_image1) was multiplied by image 2 which was obtained using the logical AND operator on the two ratioed images (band 2/band 4 and band 2/band 5). The file was named 2002_image2_cldrmv_add1_times_mask_3classes_final. As for the 1992 images, both Images 1 and 2 for 2002 have data type of integer. The multiplication of the two images was performed using the Overlay window. The result of multiplying images 1 and 2 is shown in Figure 55 (filename is 2002_image1cldrmv_times_image2).



Figure 55: 2002 Image Derived from Multiplying Images 1 and 2

Before conversion to a vector file, it was decided to reclassify the image so that only three values occur. The background was reclassified to show a value of 0. Land was assigned a value of 1 and water a value of 10.

The resulting file (2002_final_binary_image_cldrmv_reclass; see Figure 56) has a data type of byte. The file was ready for conversion from a raster to a vector file.

Since the version of Idrisi used had no advanced editing features (CartaLinx is an add on module) and the Update module in Idrisi was based on selecting specific rows and

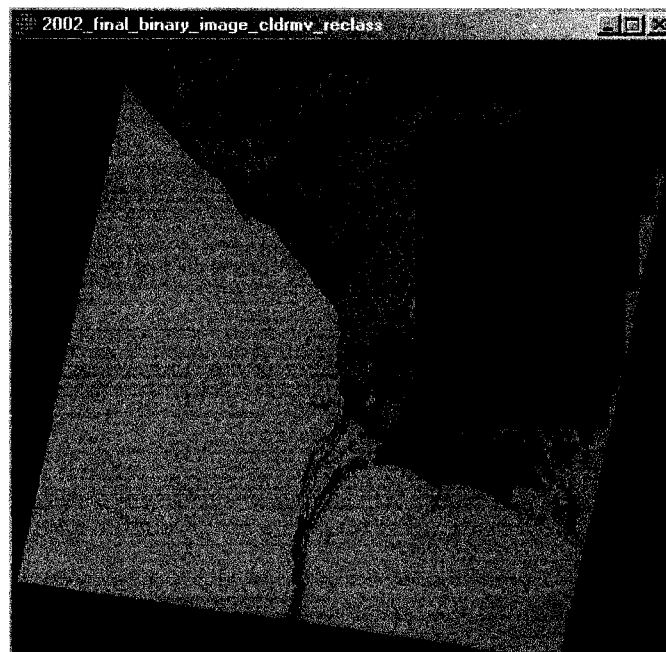


Figure 56: 2002 Final Image File Ready for Conversion to a Vector File

columns for editing, it was decided to export the raster images from Idrisi as Geotiff files for use in editing in ArcMap using the extension ArcScan.

4.2.6 Raster Clean Up Using ARCSCAN

1992

The raster image for 1992 (1992_final_binary_image_reclass) was exported from Idrisi as a GeoTiff image file. The exported image is shown in Figure 57. A personal geodatabase relating to the 1992 image was created using ArcCatalog. The raster image was imported to the geodatabase for the 1992 image using ArcCatalog. The raster image is then added to ArcMap. The 1992 composite image exported from Idrisi was also added to ArcMap. ArcScan was then used because it is a raster to vector conversion extension for ArcMap.



Figure 57: Raster Image for 1992

ArcScan operates on images which are bi-level. This means that the raster image can only have two colors visible. The objective is to have 2 classes: one representing

water, the other representing land (and the background). For the 1992 image, the values 0 and 1 (background and land) would be in one class, and 10 (water) would be in a second class. Figure 58 is the 1992 image with 2 colors.



Figure 58: 1992 Image Showing 2 Colors, One for Land (combined with the background), One for Water

Raster cleanup was begun by selecting Start Cleanup from the Raster Cleanup menu on the ArcScan toolbar. This enabled the other choices on the Raster Cleanup menu (see Figure 59). From the Raster Cleanup menu, the most frequently used choices were Fill Selected Cells and Save.

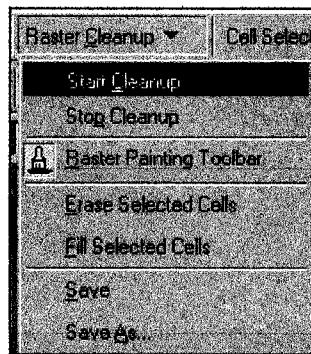


Figure 59: Raster Cleanup Menu

An example of the cleaned raster for 1992 is shown in Figure 60.

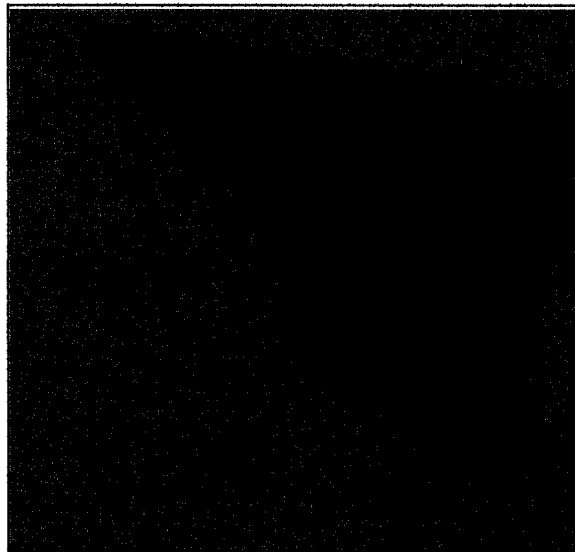


Figure 60: Cleaned Raster Image for 1992

Once the cleanup was satisfactory, Vectorization Settings was selected from the Vectorization menu.

Since ArcScan was used to automatically generate vector-based features for the 1992 image, both an empty polygon layer and an empty line layer were prepared (i.e., empty layers were placed in the geodatabase for the 1992 image).

The two previously created empty layers contained the new polygon and line layers generated by ArcScan. The line layer did not contain any information. The polygon layer contained a valid set of polygons. This feature layer had been given the filename of Shoreline_1992 and is shown in Figure 61.

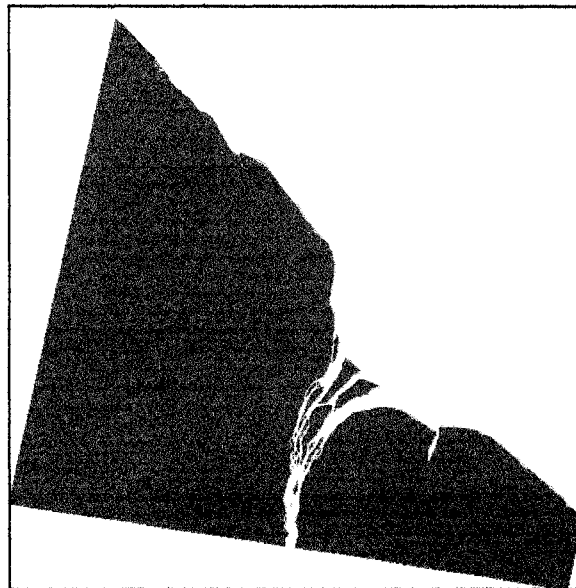


Figure 61: Vector File Showing Land Polygons for 1992

2002

The raster image for 2002 (2002_final_binary_image_reclass) was also exported from Idrisi as a GeoTiff image file. This exported image is shown in Figure 62.

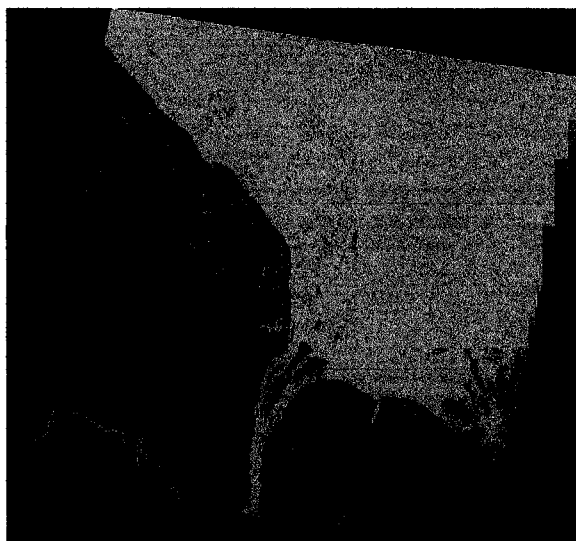


Figure 62: Raster Image for 2002

As for the 1992 image, the important objective was to distinguish land from water. A suitable color scheme was chosen for the two classes. The resulting image is shown in Figure 63. As done with the 1992 image, the objective was to cleanup the raster image



Figure 63: 2002 Image Showing 2 Colors, One for Land (combined with the background), One for Water

by removing the cloud areas, and/or misclassified pixels. The cleaned raster image for 2002 is shown in Figure 64.

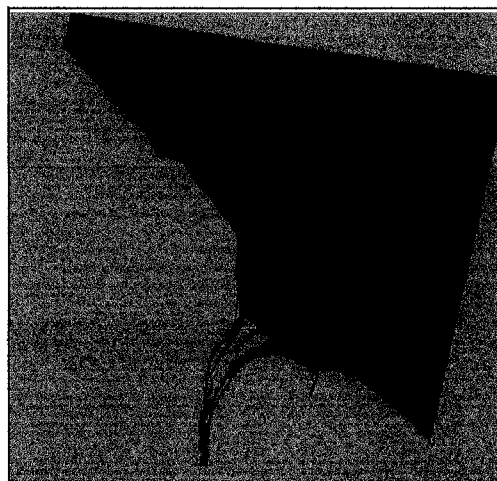


Figure 64: Cleaned Raster Image for 2002

As for the 1992 image, the line layer contained no information, and the polygon layer contained valid polygons. The feature layer had been given the name of Shoreline_2002, and is shown in Figure 65.

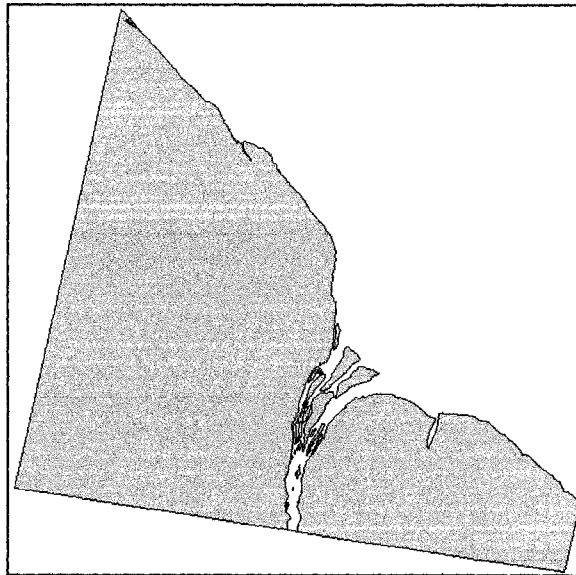


Figure 65: Vector File Showing Land Polygons for 2002

4.2.7 Prepare New Feature Layers for Difference Imaging

Two feature layers were prepared, Shoreline_1992 and Shoreline_2002. As can be seen in Figures 61 and 65, only polygons representing land are shown. A difference image involves subtraction. In order to detect areas of erosion (-1), accretion (1) and no change (0), a polygon representing water is required for both layers. In this manner, the 2002 layer can be subtracted from the 1992 and areas of change can be determined.

Add Water Polygon

The mask file used in Idrisi was exported as a GeoTiff image and added to ArcMap. The mask file was projected to the UTM Zone 20N coordinate system, the same coordinate system as for the layer files. The filename used was Mask_File_Projected. The ArcToolbox tool, RasterToPolygon was used to convert the mask file to polygons.

The Union tool was used to combine the Mask_for_1992 layer with the Shoreline_1992 layer. The resulting layer was named Shoreline_1992_Union, and is shown in Figure 66. The layer, Shoreline_2002_Union was done in a similar manner and is shown in Figure 67.

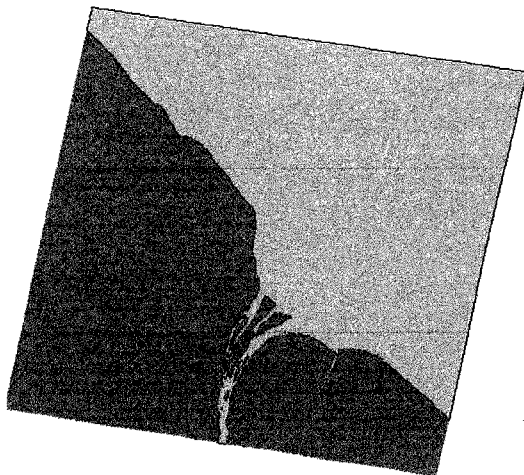


Figure 66: Shoreline_1992_Union
Showing Water Polygon

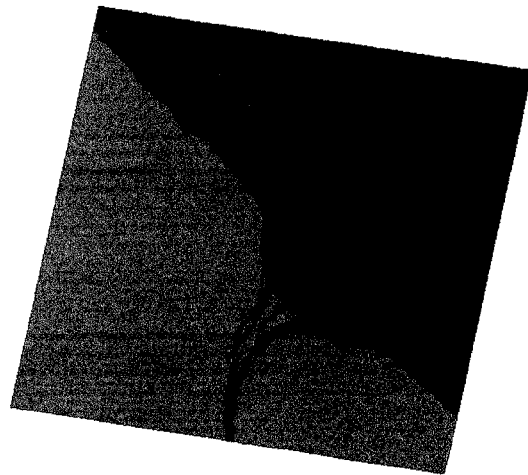
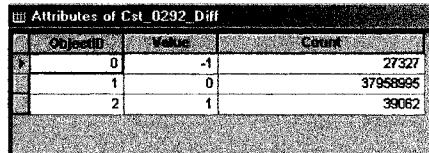


Figure 67: Shoreline_2002_Union
Showing Water Polygon

Differencing

Spatial Analyst was used to subtract the 1992 image from the 2002 image. Spatial Analyst operates on raster images. Therefore, the two layers, Shoreline_1992_Union and Shoreline_2002_Union were converted to raster images in order to obtain a difference image using Spatial Analyst.

For a difference image, one image (Shore_1992) was subtracted from another image (Shore_2002). The attribute table for the difference image is shown in Figure 68.



ObjectID	Value	Count
0	-1	27327
1	0	37958995
2	1	39062

Figure 68: Attribute Table for Difference Image. 1 represents accretion, 0 represents no change, and -1 represents erosion.

As can be seen, the attribute table contains 3 polygons. Land (2) minus water (1) equals accretion (1). Land (2) minus land (2) equals no change (0). Water (1) minus land (2) equals erosion (-1).

A portion of the attribute table for Coast_02_Diff_92 is shown in Figure 69. The Value field in the raster image is equivalent to the Gridcode in the feature layer.

To add the value, "Erosion", to all records with a Gridcode of -1, it was necessary to select only those records with the Gridcode of -1. Similarly, "Accretion" was the value

added to all records with a Gridcode of 1, and “No change” was the value added to all

Attributes of Coast_02_Diff_92				
OBJECTID	Shape	GRIDCODE	Shape_Length	Shape_Area
1	Polygon	-1	106.888886	520.145849
2	Polygon	1	4853.075055	154828.026752
3	Polygon	1	113.999872	812.248178
4	Polygon	1	113.999872	812.248178
5	Polygon	1	113.999872	812.248178
6	Polygon	1	113.999872	812.248178
7	Polygon	1	107.528907	556.139874
8	Polygon	-1	107.528276	556.133476
9	Polygon	-1	114.000898	812.262789
10	Polygon	-1	113.999872	812.248178
11	Polygon	-1	113.999872	812.248178
12	Polygon	-1	113.999872	812.248178
13	Polygon	-1	113.999872	812.248178
14	Polygon	-1	113.999872	812.248178
15	Polygon	-1	113.999872	812.248178
16	Polygon	-1	624.704758	9915.583523
17	Polygon	-1	1581.984650	124223.089814
18	Polygon	-1	1179.461925	82757.038361

Figure 69: Portion of Attribute Table Showing Gridcode (-1 represents erosion and 1 is indicative of accretion).

records with a Gridcode of 0.

5.0 RESULTS AND DISCUSSION

The GIS analysis pertaining to shifts in coastline positions could be observed by examining areas of accretion and erosion along the length of the coastline for the two time periods. The output map presented in Figure 70 and its enlarged version (Figure 70a) highlights areas where the coastline has shifted over time. While these areas are not easily

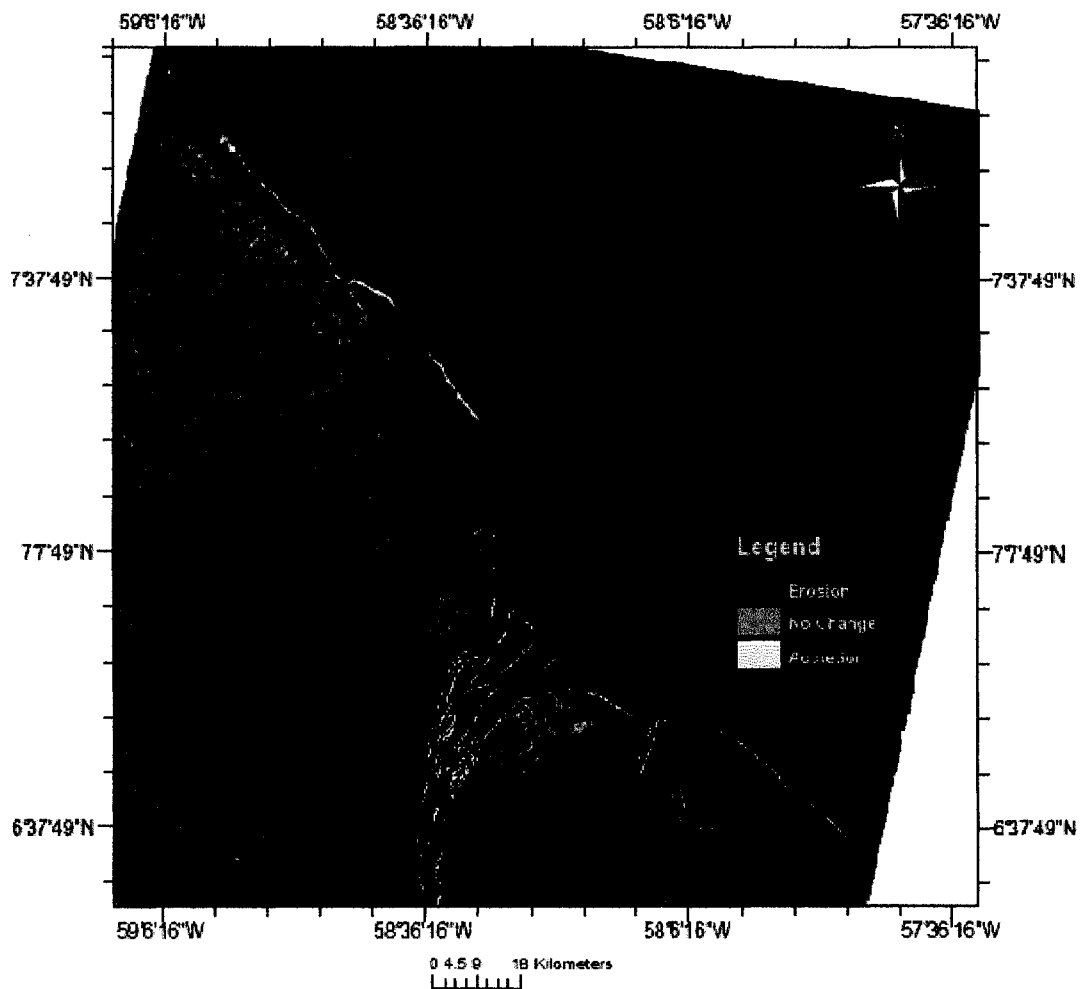


Figure 70: Areas of Erosion and Accretion along the Guyana Coast

distinguishable in Figures 1 and 1a, ArcGIS was used to produce larger scale maps to highlight those areas where coastline shifts could be easily observed.

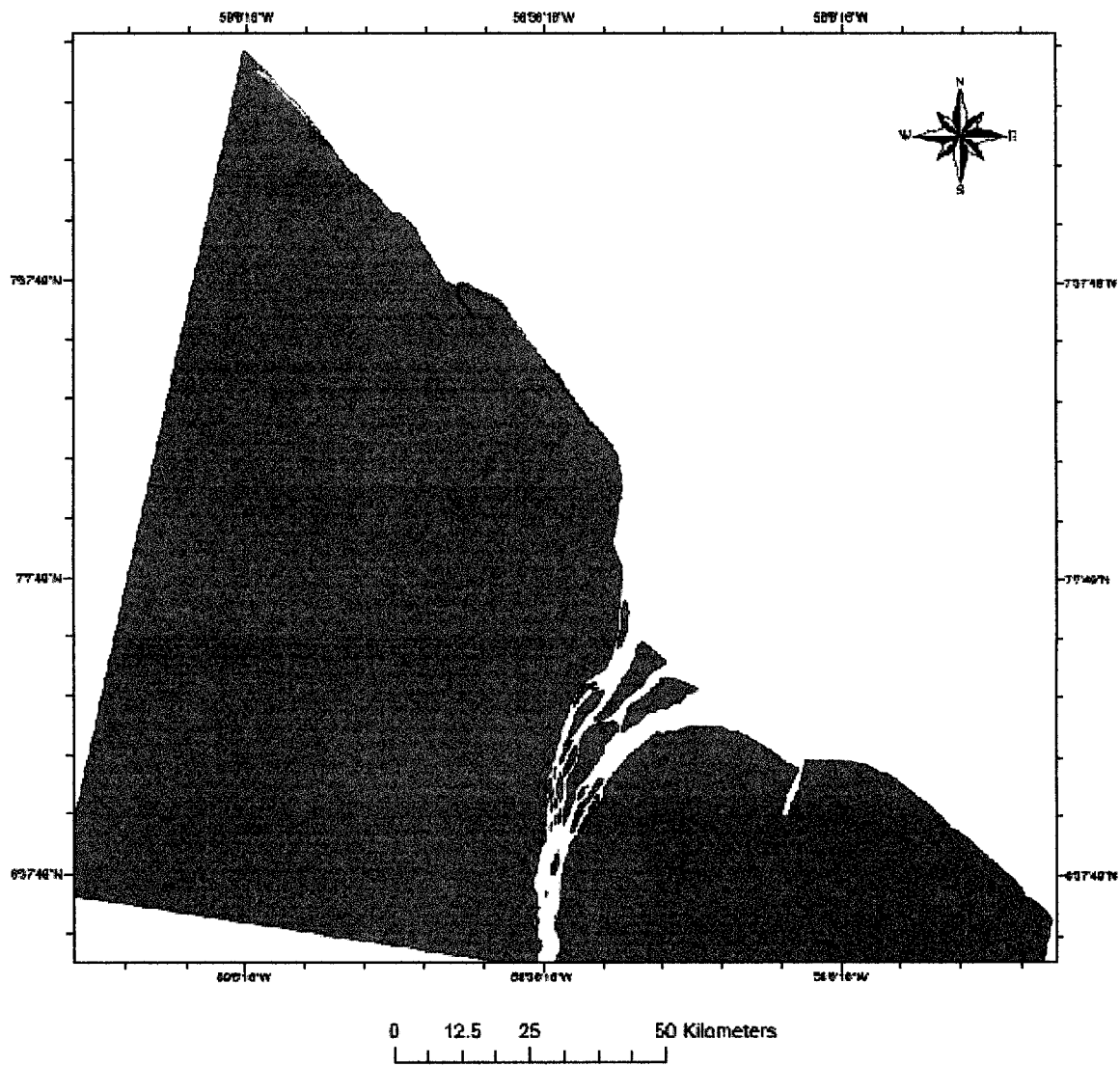


Figure 70a: Areas of Erosion and Accretion along the Guyana Coast (enlarged version)

In the upper northwest corner of the Guyana coast there is a broad band of erosion which occurred between the time period 1992 and 2002 (see Figure 71). This erosion resulted in the retreat of Papaw Beach and Ille Beach. On Figure 71 there is also a narrow

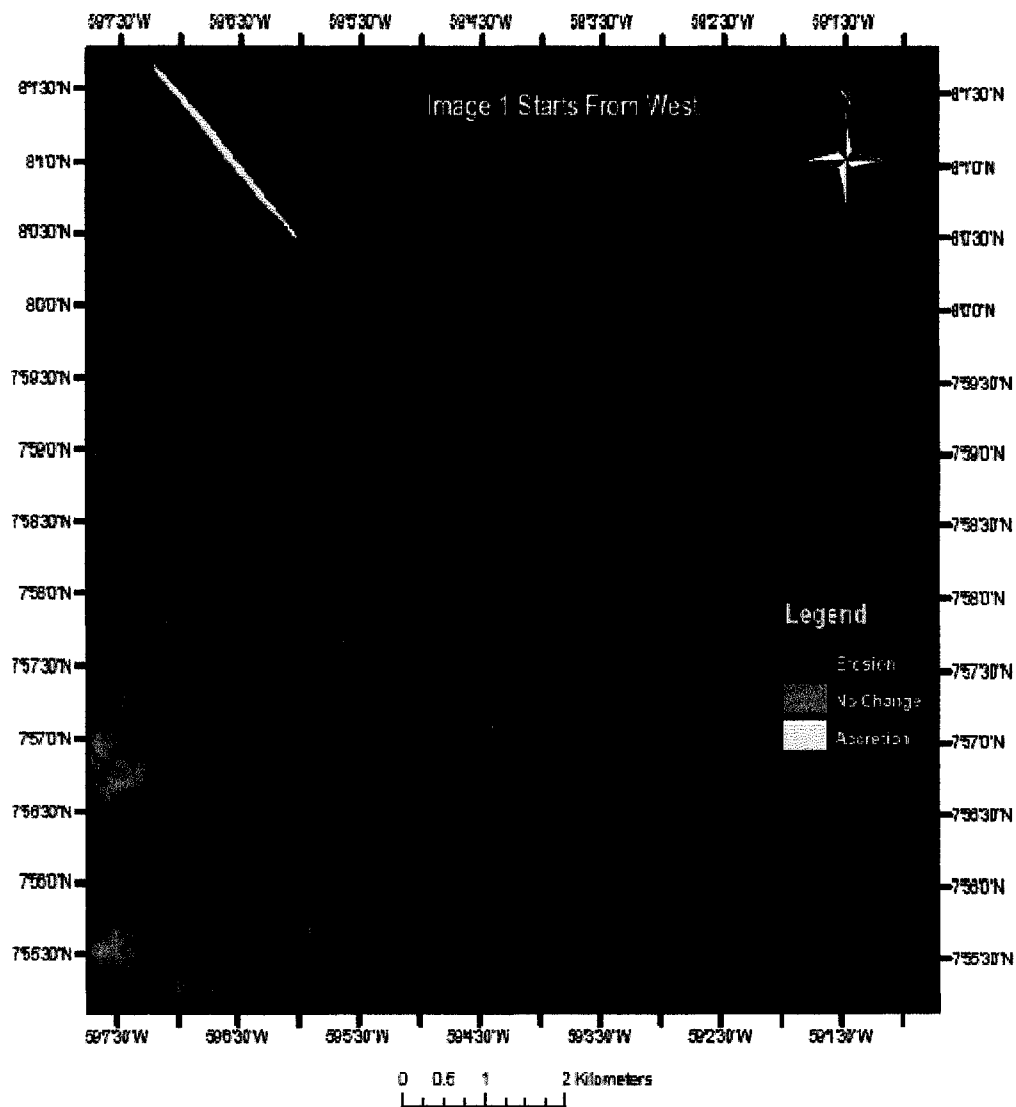
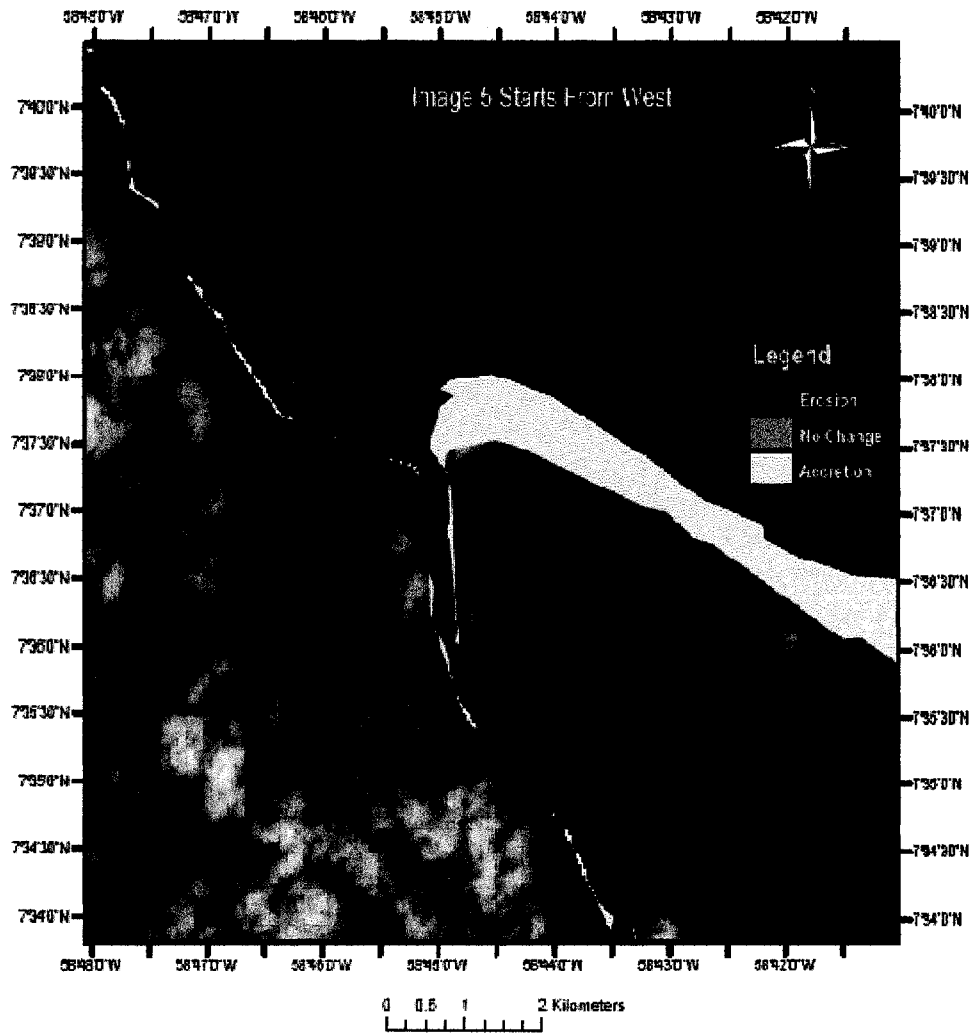


Figure 71: Erosion of Papaw Beach and Ille Beach between 1992 and 2002

accretionary area in the extreme upper northwest corner.

Beginning at the mouth of the Pomeroon River and extending almost 6 km on the eastern side is a major accretionary band of sediments (see Figure 72). This broad band of sediments almost half a kilometer wide extended to the community of Aberdeen and could be attributed to the establishment of a sandbank.



Adjoining this accretionary area is a fairly lengthy section of the coastline which

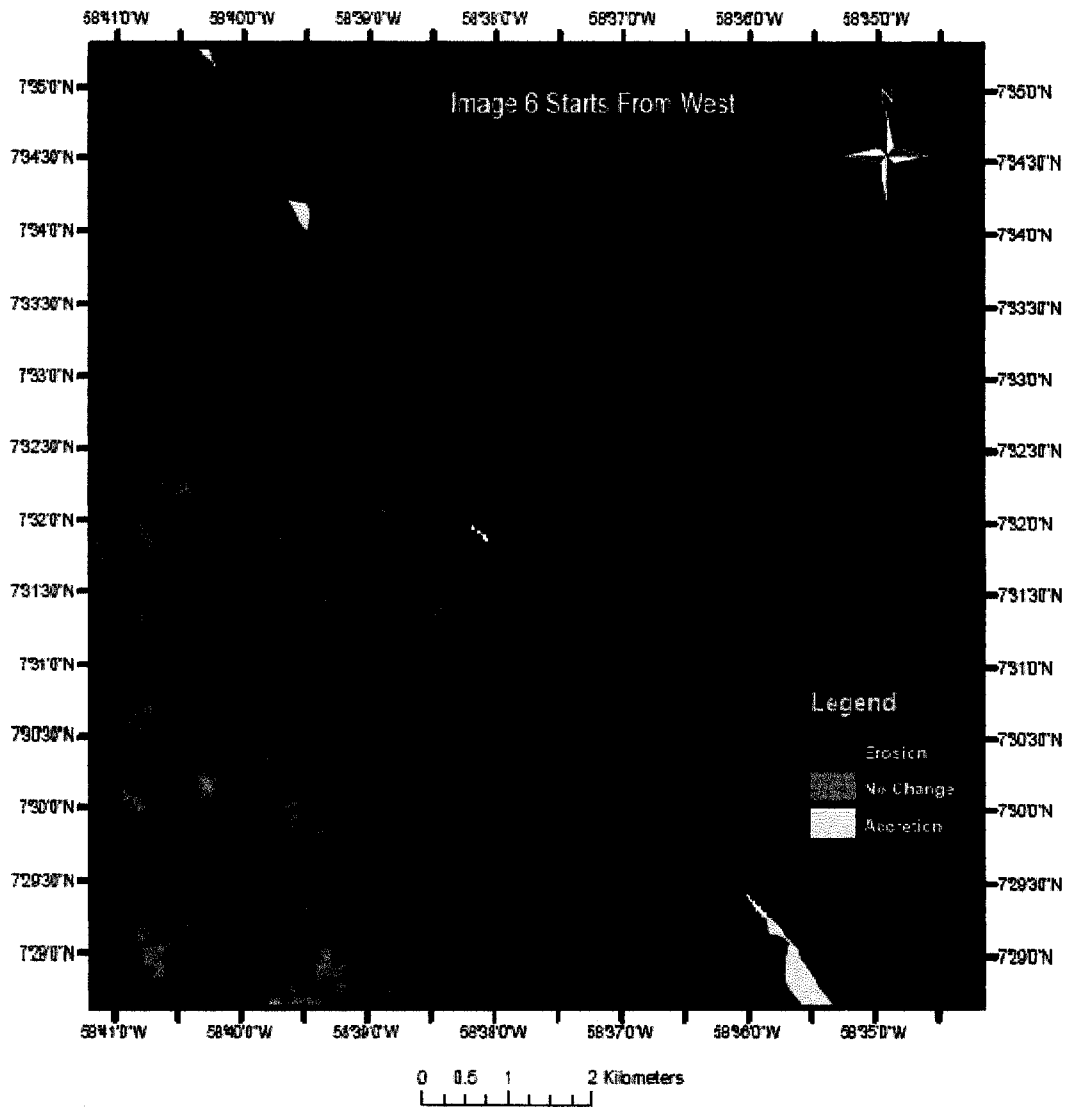


Figure 73: Coastal Erosion Zone, Freetown to Land of Promise

exhibited erosional characteristics (see Figure 73). In 2002, the coast stretching from the community of Freetown to the community of Land of Promise was under intense

wave-induced erosion.

This alternating patterns of accretion and erosion are again observed along the coast where on the western side of the mouth of the Essequibo River there is also a distinct accretionary area which stretched for nearly 20 km along the coast (Figure 74).

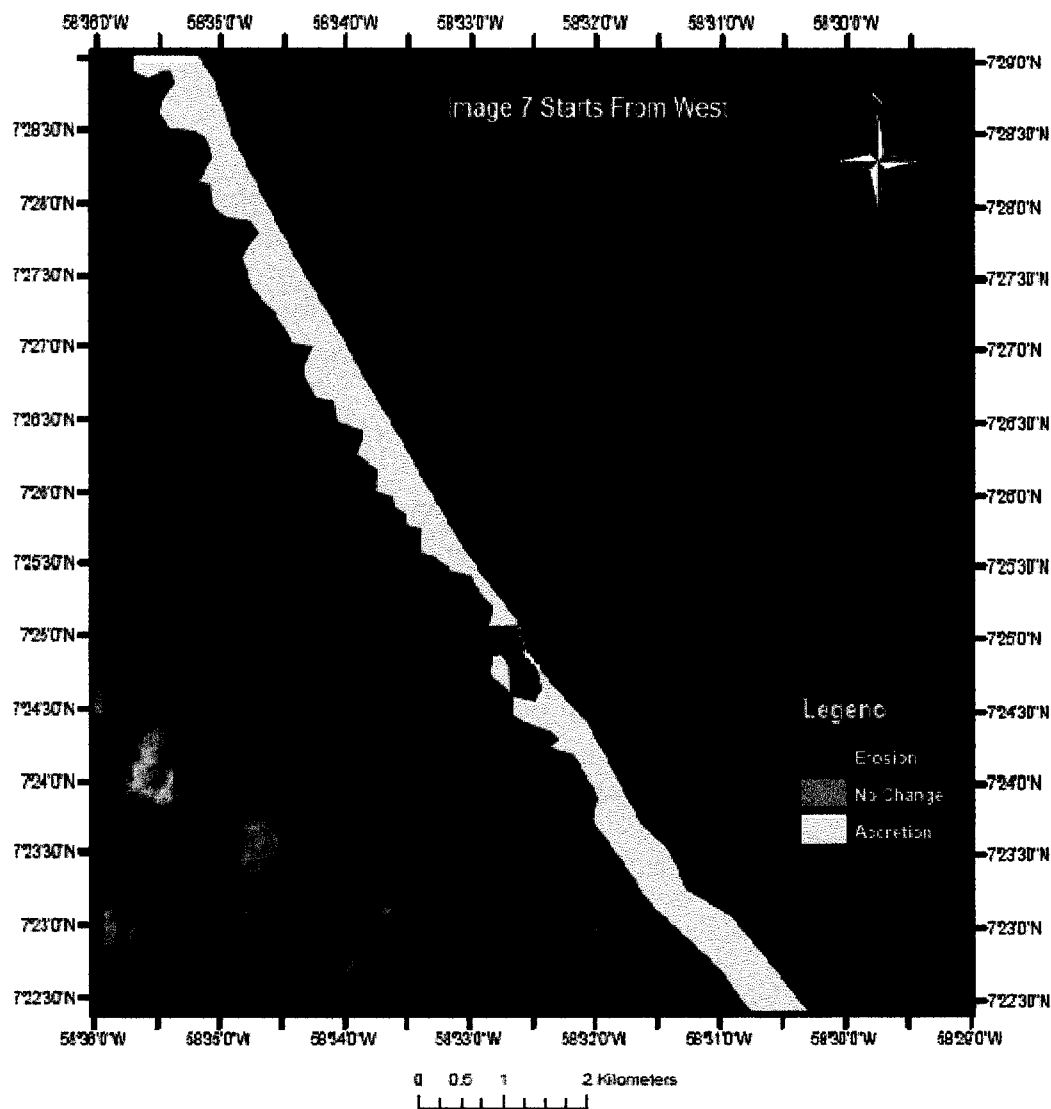


Figure 74: Accretion Zone found along western side of the mouth of the Essequibo River

The entire area from Playfair to Charity was associated with accretional characteristics. Along the coast away from the Essequibo River there are small but evident linear bands of accretion and erosion.

The distinct accretionary area along the Demerara coast, from the community of Paradise to Ann's Grove (Figure 75), was observed in 2002 by field researchers from the University of Windsor. This is then followed by a noticeable erosional trend along the coastline (Figure 76). The erosional area, from Clonbrook to Concord, was in the same locality which was being studied by graduate students from the University of Windsor. Interestingly, the positional shifts of the coastline recorded by remote sensors are in very close agreement with those of field observations.

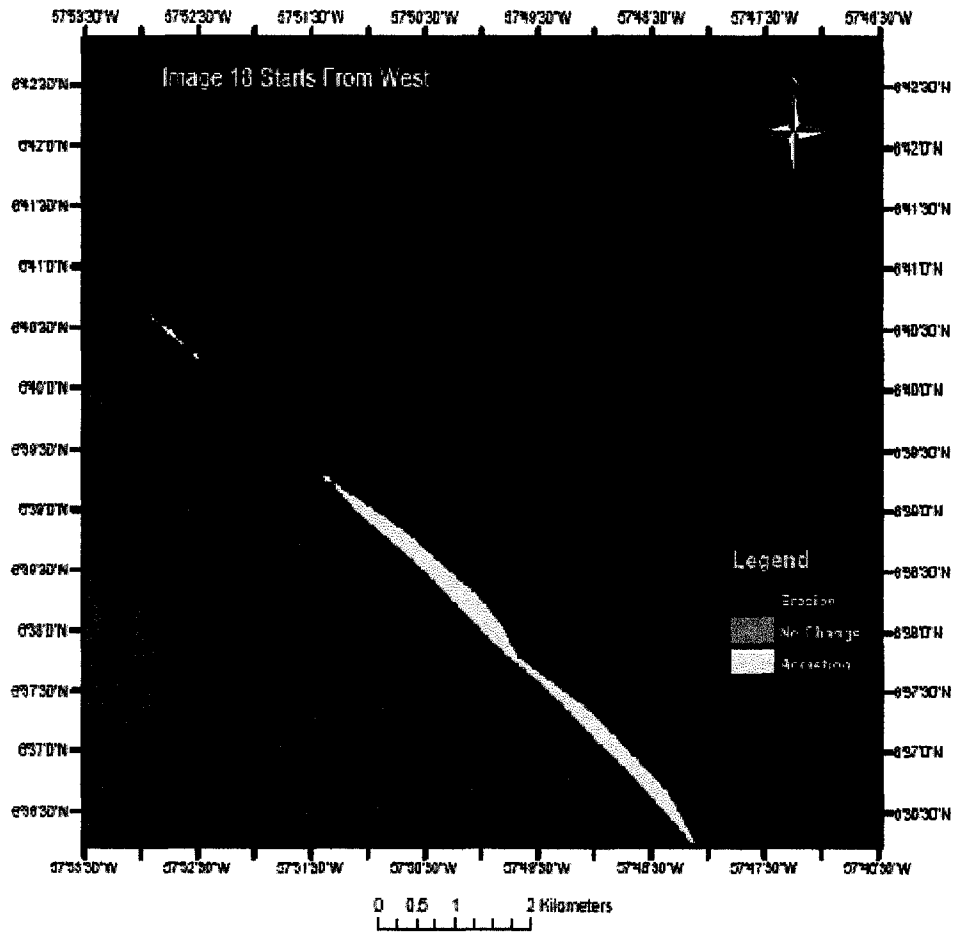


Figure 75: Accretionary Area, from the community of Paradise to Ann's Grove

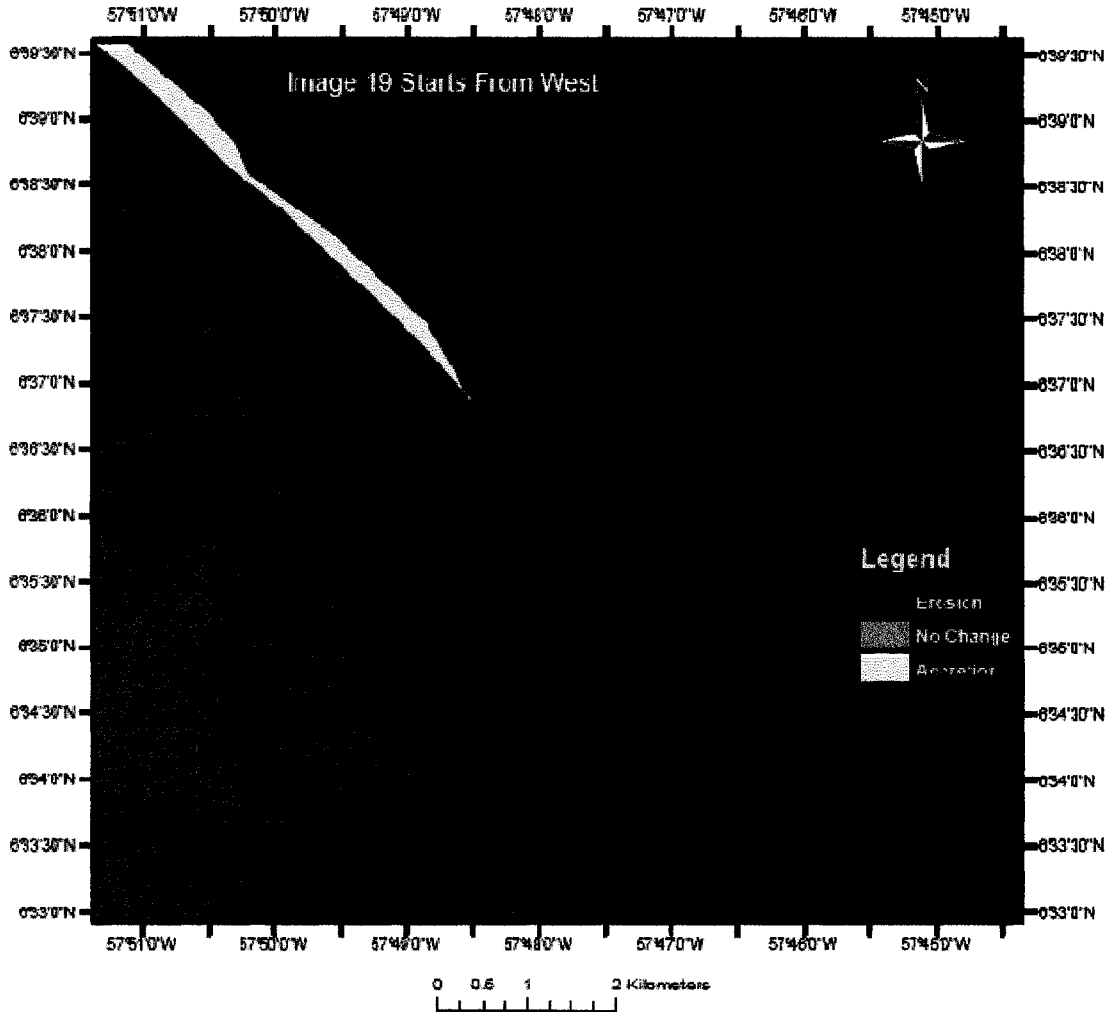


Figure 76: Accretion Areas, from Clonbrook to Concord.

Given the distinct areas of erosion and accretion which have been observed in the two time periods, the claim could be made that the procedures used in this study have permitted the recognition and delineation of spatial areas along the Guyana coastline which have experienced positional shifts. Evidently, the coast is of a dynamic nature where there are alternating spatial areas of accretion and erosion.

A tabulation of the polygons which have been identified as either accretional or erosional demonstrates that the entire coastal area is one where either erosion or accretion is occurring. When the ArcGIS-generated polygons are tabulated in an Excel spreadsheet it was found that there were 2 098 accretional polygons and 2 109 erosional polygons. Only 14 polygons indicated areas of no change. These results are plotted in Figure 77. Evidently, the coast displays distinct temporal phase shifts. These shifts occur at various

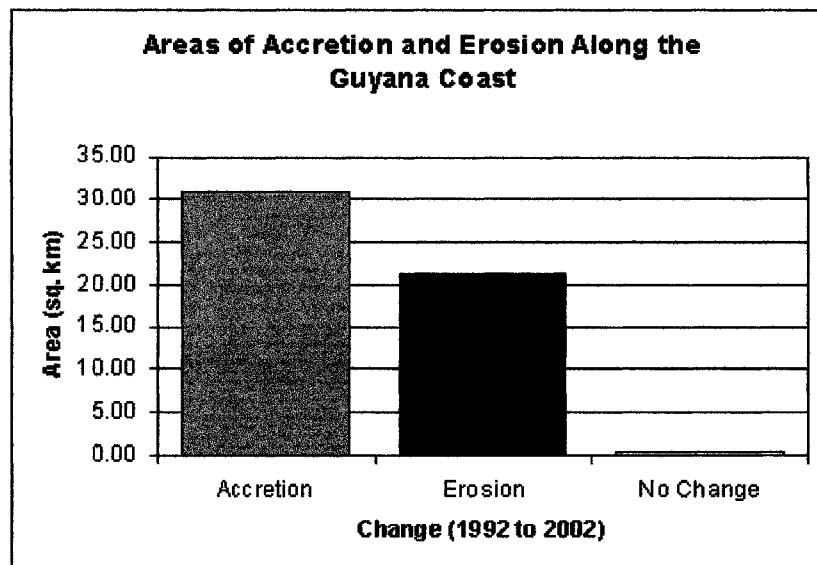


Figure 77: Areas of Accretion and Erosion Along the Guyana Coast

spatial scales. The analysis of empirical data by Lakhan et al. (2004; 2006) highlighted the fact that the Guyana coast, at different spatial scales and at different times, will display quantifiable aggradational and degradational sequences. Given the fact that temporal patterns of accretion and erosion have a direct influence on the morphological stability and positional shifts of the coastline it becomes vital to understand and predict these positional shifts. The results of this study provide adequate evidence that the use of remote sensing imagery can make a substantial contribution to understanding, on a timely basis, the dynamic nature of the Guyana coast.

6.0 CONCLUSION

The need to provide an ongoing and comprehensive management plan for the coastal zone of Guyana is apparent given the dynamic nature of this environment and its reliance on coastal resources for its inhabitants. In order to provide timely and accurate coastal data for coastal investigators, the incorporation of Landsat TM and ETM+ imagery in the extraction of the Guyana coast served to fulfil the objectives established in this thesis; namely:

- (1) remote sensing techniques as outlined in the methodology successfully delineated coastline positions for the 1992 and 2002 time periods;
- (2) spatial and temporal changes that occurred along the Guyana coast were readily visualized given the mapped outputs; and
- (3) areas of erosion and accretion were identified, visualized and quantified through the incorporation of remote sensing techniques and a GIS.

The use of the imaging processing techniques presented in the methodology provided the necessary framework for the successful extraction of the coastlines. The selection of the mid-infrared band within the electromagnetic spectrum (TM and ETM+) provided the best spectral response for delineating the water-land interface. The combination of contrast stretching and histogram thresholding of band 5 readily identified the necessary threshold values in the analysis. This coupled with band ratioing of bands 2 and 4, and bands 2 and 5 enhanced the differences in spectral reflectance to establish the binary classification.

The incorporation of both methods through image multiplication served to

demarcate the coastlines for subsequent vectorization, and calculation of accretional and erosional areas. The use of ARCVIEW GIS provided the necessary framework for raster to vector conversions using the extension ArcScan which provided the polygon based maps to visual change along the coast. The overlay analysis employed within this study to quantify lineal change was performed through the Spatial Analyst extension. The ability to convert the data back from vector to raster images permitted the calculation of change polygons denoting erosion, accretion or no change. The utility and flexibility of the ARCVIEW GIS software program was invaluable in visualizing, assessing and quantifying shoreline positional change for this study.

The synoptic view provided by the results clearly show that the coast of Guyana experiences a dynamic framework of alternating areas of erosion and accretion. The ability to visual and quantify areas of erosion and accretion were evident through the overlay analysis provided (Figure 70-76). When examining Figure 77, the results clearly indicate the instability of the coast over time period 1992 to 2002. The morphological change that occurred is indicative of an overall balance along the coast as noted by the changing position of the coastline and its corresponding area of change (Figure 77). In the analysis, the evolution of the coast of Guyana displays temporal shifts at different spatial scales. The synoptic view provided for the 170 km portion of the Guyana coast was beneficial in showing large scale change over the ten year time period.

The observed alternating pattern of erosion and accretion resemble a sawtooth pattern along the 170 km stretch of the Guyana coast. Given this pattern and the empirical evidence supported by Lakhan *et al.* (2004; 2006), cyclical trends in erosion

and accretion patterns have occurred. This may help to explain the movement of available material from an area of erosion to an accretionary zone further along the coast. Further evidence indicates that the Demerara coast experiences predictable patterns of erosion and accretion based on observations spanning four decades. The latest erosion and accretion patterns reflected during the 1982-1987 observations showed an erosional cycle. The results from this study reveal an alternating pattern of an accretionary cycle along the Demerara coast for the 1992-2002 time period. The observed shift in shoreline position and resulting spatio-temporal changes associated with the aforementioned pattern may be indicative of quasi-stationary circulation cell affecting the Guyana coast.

Additionally, the formation and presence of mudbanks adjacent to the coast have known to affect the morphology and configuration of the shoreline. It is known that mudbanks dampen the effect of propagating waves against a coast (Allersma, 1971; Augustinus, 1987; Lakhan and Pepper, 1997), and as a result, accretion occurs along the coast adjacent to the mudbank. Conversely, coastal areas experience erosion when mudbanks are absent in attenuating wave energy upon a coast. The repeated pattern of mudbank migration and stabilization affect the spatio-temporal changes associated with erosion and accretion patterns (Lakhan and Pepper, 1997). Based on this information, mudbanks affect littoral cell circulation and their associated velocity patterns and ultimately contribute to the alternating patterns of erosion and accretion observed in this study.

Although the extraction of coastlines for the time periods 1992 and 2002 was successfully accomplished, there were, nevertheless, certain limitations. Primarily, this

method of coastline extraction is reliant upon a series of algorithms inherent to the Idrisi software package. A series of preprocessing, radiometric and geometric corrections, and image enhancement steps were used to calibrate images, enhance contrast within an image through stretching and band ratioing, reclassify image data based on initial radiant values or DN_s, and produce raster and vector files for demarcation of the coastline.

Given the nature and complexity of the mathematics involved within the application of these algorithm-based modules it is difficult to ascertain a true truncation point that would ultimately define the water's edge. Best estimates and segmentation averages within the sections of the coastline were subjected to line smoothing techniques which served to assign the midpoint value of vector files representing the coastline. These methods coupled with a resolution of 30 m from the Landsat images can not produce digital quality photographs of coastlines when compared to more contemporary finer resolution satellite platforms of IKONOS and Quickbird with 1 m resolution capabilities.

Furthermore, the nature of the resolution of TM and ETM+ images produces mixed pixels that reflect an area of both land and water that may be manifested within a tidal flat or nearshore turbidity. As a result, average brightness values expressed as DN_s within a pixel may not be a true representation of the ground features found along the Guyana coast. To circumvent this issue, histogram thresholding was employed on Bands 5 to ascertain the threshold value representing the land-water interface by segmenting pixels into either a water or land class. However, when examining a typical histogram within any TM or ETM+ band the visual interpretation of the saddle point found between

the twin peaks is chosen arbitrarily. Hence, the exact value is determined by the user from area to area and is dependent upon the user's level of expertise in image classification and knowledge of the local area (Ouma and Tateishi, 2006). Conceptually, this arbitrary classification found within the narrow band of the histogram valley may overestimate water pixels or land pixels given the spectral response of each class along the coastline.

While many areas of accretional and erosional changes were recognized with the remote sensing images, only a few could be compared with data collected from the coast of Guyana. Interestingly, the morphological changes observed through analysis of the remote sensing images are similar to those documented by Lakhan et al. (2004) for a 30-km portion of the coastline. Unfortunately, empirical data do not exist to verify the positional changes observed by the remote sensing sensors in the various other spatial locations along the coast. This limitation could be rectified with an ongoing and timely field program which monitors morphological changes throughout the length of the coast. Lastly, slight variations in tidal ranges between the 1992 and 2002 images within the relatively flat plain of the Guyana coast may result in the underestimation of water or land pixels and its corresponding measure of accretion or erosion.

The use of Landsat TM and ETM+ images, together with the automatic extraction method presented in this study will serve as a reliable, efficient and cost effective method to detect coastline positional changes. The computer-assisted capabilities of this method will allow coastal investigators to visualize and quantify lineal changes that occur along the coastline fairly rapidly. Having knowledge of areas of accretion and erosion will

permit investigation by coastal researchers. Given this ancillary information, coastal zone planners and managers will acquire the necessary information to make informed and coordinated decisions to assess the level of vulnerability of coastal areas, and specifically to provide the appropriate management response. In the final analysis this method of coastline extraction will serve to facilitate the interests of all stakeholders in the protection and management of coastal resources.

REFERENCES

- Ahmad, A.A.Z., 1994. Remote Sensing and GIS Application in Coastal Zone Management and Water Resources. *Ecodecision*, January, 79-80.
- Ahmad, S.R., Lakhan, V.C., and Karki, R., 2005. GIS-based modelling and prediction of coastline positional change along the Demerara coast. *Journal of Indo Caribbean Research*, 6(1): 75-87.
- Alesheikh, A.A., Ghorbanali, A., and Talebzadeh, A., 2004. Generation of a coastline map for Urmia Lake by TM and ETM+ imagery. *GIS Development*, PERLINK"<http://www.gisdevelopment.net/applications/nrm/coastal/mnm/ma04022.htm>"www.gisdevelopment.net/applications/nrm/coastal/mnm/ma04022.htm (accessed September 13, 2006)
- Allersma, E., 1971. Mud on the Oceanic Shelf off Guiana. Symposium of Investigations and Resources of the Caribbean Sea and Adjacent Regions. UNESCO, France: Imprimerie Louis-Jean pp. 193-203.
- Al-Tahir, R., and Ali, A., 2004. Assessing Land Cover Changes in the Coastal Zone Using Aerial Photography. *Surveying and Land Information Science*, 64(2): 107-112.
- Alves, A.L., Amaro, V.E., and Vital, H., 2003. Multitemporal Analysis of Multispectral Landsat 5 - Thematic Mapper Images for Monitoring and Evaluation of Coastal Morphodynamic on the Northeastern Coast of Brazil. *Journal of Coastal Research*, SI (35): 279-283.
- Anthony, E.J., Gardel, A., Dolique, F., and Guiral, D., 2002. Short-term Changes in the Plan Shape of a Sandy Beach in Response to Sheltering by a Nearshore Mud Bank, Cayenne, French Guiana. *Earth Surface Processes and Landforms*, 27: 857-866.
- Augustinus, P.G.E.F., 1987. The Geomorphological Development of the Coast of Guyana Between the Coretyne River and Essequibo River. In: Gardiner, V. (Editor), *International Geomorphology*, 1986. Part 1. Utrecht, The Netherlands: Wiley, pp. 1281-1293.
- Bagli, S. And Soille, P., 2004. Automatic delineation of shoreline and lake boundaries from Landsat satellite images. *Proceedings of initial ECO-Imagine GI and GIS for Integrated Coastal Management, Seville, Spain, May 13th-15th, 2004.*

- Brock, J.C., Wright, C.W., Sallenger, A.H., Krabell, W.B., and Swift, R.N., 2002. Basis and Methods of NASA Airborne Topographic Mapper Lidar Surveys for Coastal Studies. *Journal of Coastal Research*, 18(1): 1-13.
- Cambers, G., 1975. Temporal scales in coastal erosion systems. *British Geographers, Transactions New Series*, Volume, 1, No. 2: 246-256.
- Clark Labs, 2003. *Idrisi Kilimanjaro 14.002*. Clark University, Worcester, MA.
- Crowell, M., Leatherman, S.P., and Buckley, M.K., 1991. Historical Shoreline Change: Error Analysis and Mapping Accuracy. *Journal of Coastal Research*, 7(3): 839-852.
- Dolan, R., Fenster, M.S., and Holme, S.J., 1991. Temporal Analysis of Shoreline Recession and Accretion. *Journal of Coastal Research*, 7(3): 723-744.
- Environmental Research Systems Institute (ESRI), 2001. ARC VIEW GIS version 9. ESRI, Redlands, CA.
- Fenster, M.S., Dolan, R., and Elder, J.F. 1993. A New Method for Predicting Shoreline Positions from Historical Data. *Journal of Coastal Research*, 9(1): 147-171.
- Fletcher, C., Rooney, J., Barbee, M., Siang-Chyn, L. and Richmond, B., 2003. Mapping Shoreline Change Using Orthophotogrammetry on Maui, Hawaii. *Journal of Coastal Research*, Special Issue (38): 106-124.
- Foster, E.R. and Savage, R.J., 1989. Methods of Historical Shoreline Analysis. *Coastal Zone '89*. New York: American Society of Civil Engineers, pp. 4434-4448.
- Gardner, N., 1992. Remote Sensing. In *The Student's Companion to Geography*, 151-159. Rogers, A. *et al.*, (eds.). Oxford: Basil Blackwell.
- Grigio, A.M., Amaro, V.E., Vital, H., and Diodato, M.A., 2005. A Method for Coastline Evolution Analysis Using GIS and Remote Sensing - A Case Study from the Guamare City, Northeast Brazil. *Journal of Coastal Research*, SI (42): 412-421.
- Jensen, J.R., 1996. *Introductory Digital Image Processing: A Remote Sensing Perspective*. Prentice-Hall: New Jersey.
- Jiménez, J.A., Sanchez-Arcilla A., Bou J. and Ortiz M., 1997. Analysing Short-Term Shoreline Changes Along Erbo Delta (Spain) Using Aerial Photographs. *Journal of Coastal Research*, 13(4), Fall: 1256-1266.

- Klemas, V., Dobson J., Ferguson R., and Haddad K. 1993. A Coastal Land Cover Classification System for the NOAA Coastwatch Change Analysis Project. *Journal of Coastal Research*, 9(3), Summer: 862-872.
- Lakhan, V.C., 1991. Simulating the interactions of changing nearshore water levels, morphology and vegetation growth on Guyana's coastal environment. In: McLeod, J. (Editor), *Toward Understanding Our Environment*. Simulation Councils, Inc., San Diego, CA, pp. 13-20.
- Lakhan, V.C., 1993. Image Processing Techniques to Evaluate Actual and Potential Degradation of Guyana's Coastal Wetlands. Commonwealth Geographical Bureau Congress, August 13-29, 1993, University of Guyana, Georgetown, Guyana. Manuscript, 47p.
- Lakhan, V.C., 1994. Planning and Development Experiences in the Coastal Zone of Guyana. *Ocean and Coastal Management*, 22: 169-186.
- Lakhan, V.C., 2005. Proposed Framework for the Implementation of a Spatial Decision Support System for Coastline and Flood Prediction Along the Guyana Coast. *Journal of Indo Caribbean Research*, 6: 17-35.
- Lakhan, V.C., Ahmad, S.R., and Parizanganeh, A., 2006. Investigating Shifting Mudbanks Along a Coast Subject to Cycles of Accretion and Erosion. In: A. Tubielewicz (editor), *Eurocoast - Littoral 2006. Coastal Environment, Processes and Evolution*. Gdańsk University of Technology, Faculty of Management and Economics, Gdańsk, Poland, pp. 90-97.
- Lakhan, V.C., Cabana, K., and LaValle, PD, 2002. Heavy metal concentrations in surficial sediments from accreting and eroding areas along the coast of Guyana. *Environmental Geology*, 42: 73-80.
- Lakhan V.C., Kanyaya, J. and Karki, R., 2004. GIS analysis and time series modelling of coastal change. *Delivering Sustainable Coasts: Connecting Science and Policy*. Littoral 2004, Proceedings, Volume 2, pp. 432-437.
- Lakhan, V.C., and Pepper, D.A., 1997. Relationship Between Concavity and Convexity of a Coast and Erosion and Accretion Patterns. *Journal of Coastal Research*, 13 (1): 226-232.
- Lakhan, V.C., Trenhaile, A.S. and LaValle, PD, 2000. Environmental protection efforts in a developing country: The case of Guyana. *Electronic Green Journal*, Issue 13, <http://egj.lib.uidaho.edu/egj13/lakhan1.html>.

- Lillesand, T.M., and Kiefer, R.W., 1994. *Remote Sensing and Image Interpretation*. John Wiley and Sons: New York.
- Lillesand, T.M., Kiefer, R.W., and Chipman, J.W., 2004. *Remote Sensing and Image Interpretation*, 5th Edition. John Wiley and Sons: New York.
- Lucas, A.E., 1996. Data for Coastal GIS: Issues and Implications for Management. *GeoJournal*, 39(2): 133-142.
- McFeeters, S.K., 1996. The use of the Normalized Difference Water Index (NDWI) in the delineation of open water features. *International Journal of Remote Sensing*, 17(7): 1425-1432.
- Moore, L.J., 2000. Shoreline Mapping Techniques. *Journal of Coastal Research*, 16(1): 111-124.
- Noernberg, M.A. and Marone, E., 2003. Spatial-temporal Monitoring of the Paranagua Bay Inlet Margins Using Multispectral Landsat-TM Images. *Journal of Coastal Research*, SI(35): 221-231.
- O'Regan P.R., 1996. The Use of Contemporary Information Technologies for Coastal Research and Management – A Review. *Journal of Coastal Research*, 12(1): 192-204.
- O'Regan P.R., Morad M., and Chalmers A.I., 1995. Digital Analysis of Shoreline Change. *New Zealand Geographer*, 51(2): 25-31.
- Ouma, Y.A. and Tateishi, R., 2006. A water index for rapid mapping of shoreline changes of five East African Valley lakes: an empirical analysis using Landsat and ETM+ data. *International Journal of Remote Sensing*, 27(15): 3153-3181.
- Ryu, J., Won, J. And Min, K.D., 2002. Waterline extraction from Landsat TM data in a tidal flat - A case study in Gomso Bay, Korea. *Remote Sensing of the Environment*, 83: 442-456.
- Phillips, J.D., 1986. Spatial Variability of Shoreline Erosion, Delaware Bay, New Jersey. *Annals of the Association of the American Geographers*, 76(11): 50-62.
- Sabins, Jr., F.F., 1987. *Remote Sensing; Principles and Interpretation*. New York: W.H. Freeman.
- Scott, J.W., Moore, L.R., Harris, W.H. and Reed, M.D., 2003. Using Landsat 7 Enhanced Thematic Mapper Tasseled Cap Transformation to Extract Shoreline. *U.S. Geological Survey Open-File Report OF 03-272*.

- Singhroy, V., 1996. Interpretation of SAR Images for Coastal Zone Mapping in Guyana. *Canadian Journal of Remote Sensing*, 22: 317-328.
- Smith, G.L. and Zarillo, G.A., 1990. Calculating Long-Term Shoreline Recession Rates Using Aerial Photographic and Beach Profiling Techniques. *Journal of Coastal Research*, 6(1): 111-120.
- Turner, I.L., Aarninkoff, G.J. and Holman, R.A., 2006. Coastal Imaging Applications and Research in Australia. *Journal of Coastal Research*, 22(1): 37-48.
- White, K., and El Asmar, H.M., 1999. Monitoring changing position of coastlines using thematic mapper imagery, an example from the Nile delta. *Geomorphology*, 29: 93-105.
- Williams, D.C. and Lyon, J.G., 1997. Historical Aerial Photographs and a Geographic Information Systems (GIS) to Determine Effects of Long-Term Water Fluctuations on Wetlands along the St. Mary's River, Michigan, USA. *Aquatic Botany*, 58(3-4), October: 363-378.

VITA AUCTORIS

Name: Daniel Thomas Aquinas Fister

Place of Birth: Windsor, Ontario, Canada

Year of Birth: 1963

Education: Herman Secondary School, Windsor, Ontario
1977-1982

University of Windsor, Windsor, Ontario
1982-1985
Bachelor of Arts - Geography

Simon Fraser University, Burnaby, British Columbia
1985-1986
Minor in History

University of Windsor, Windsor, Ontario
1986-1987
Bachelor of Education - Intermediate/Senior Divisions

University of Windsor, Windsor, Ontario
1999-2007
Master of Arts - Geography